Spatiotemporal distribution of bacterial DMSP producing and catabolic genes in the Changjiang Estuary

Hao Sun[1,2], Ji Liu[1], Siyin Tan[1], Yanfen Zheng[1], Xiaolei Wang[1], Jinchang Liang[1], Jonathan D. Todd[3*] and Xiao-Hua Zhang[1,2,4*]

[1]College of Marine Life Sciences, and Frontiers Science Center for Deep Ocean Multispheres and Earth System, Ocean University of China, 5 Yushan Road, Qingdao 266003, China

[2]Laboratory for Marine Ecology and Environmental Science, Qingdao National Laboratory for Marine Science and Technology, Qingdao 266071, China

[3]School of Biological Sciences, University of East Anglia, Norwich Research Park, Norwich, NR47TJ, UK

[4]Institute of Evolution & Marine Biodiversity, Ocean University of China, Qingdao 266003, China

***Correspondence:**

Xiao-Hua Zhang, xhzhang@ouc.edu.cn; Jonathan D. Todd, jonathan.todd@uea.ac.uk

Running title: Bacterial DMSP production and catabolism in Estuary

Summary

The osmolyte dimethylsulfoniopropionate (DMSP) is produced in petagram amounts by marine microorganisms. Estuaries provide natural gradients in salinity and nutrients, factors known to regulate DMSP production, yet there have been no molecular studies of DMSP production and cycling across these gradients. Here, we study the abundance, distribution and transcription of key DMSP synthesis (*dsyB* and *mmtN*) and catabolic (*dddP* and *dmdA*) genes along the salinity gradient of the Changjiang Estuary. DMSP levels did not correlate to Chl *a* across the salinity gradient. In contrast, DMSP concentration, abundance of bacterial DMSP producers and their *dsyB* and *mmtN* transcripts were lowest in the freshwater samples and increased abruptly with salinity in the transitional and seawater samples. Metagenomics analysis suggests that bacterial DMSP-producers were more abundant than their algal equivalents and were more prominent in summer than winter samples. Bacterial DMSP catabolic genes and their transcripts followed the same trend of being greatly enhanced in transitional and seawater samples with higher DMSP levels than freshwater samples. DMSP cleavage was likely the dominant catabolic pathway, with DMSP lyase genes being ~4.3-fold more abundant than the demethylase gene *dmdA*. This is an exemplar study for future research on microbial DMSP cycling in estuary environments.

Key words: DMSP production; DMSP catabolism; spatiotemporal distribution; the Changjiang Estuary, salinity gradient.

Introduction

Dimethylsulfoniopropionate (DMSP) is one of the Earths most abundant organosulfur compounds synthesized by many marine phytoplankton (Ackman et al., 1966), macroalgae (Dickson et al., 1980; Van Alstyne and Puglisi, 2007), some angiosperms (Rhodes et al., 1997), corals (Raina et al., 2013) and heterotrophic bacteria (Curson et al., 2017) to petagram quantities annually (Ksionzek et al., 2016; Zhang et al., 2019). Three pathways for DMSP

biosynthesis from methionine (Met) have been identified, the transamination pathway in marine algae, corals and bacteria (Gage et al., 1997; Raina et al., 2013; Curson et al., 2017), the methylation pathway in angiosperms and bacteria (Rhodes et al., 1997; Kocsis and Hanson, 2000; Williams et al., 2019), and the decarboxylation pathway in one dinoflagellate (Uchida et al., 1996).

Recent molecular studies have identified key *S*-methyltransferase encoding genes of the Met transamination (methylthiohydroxybutryrate (MTHB) *S*-methyltransferase, *dsyB*) and Met methylation (Met *S*-methyltransferase, *mmtN*) pathways for DMSP synthesis in marine bacteria (Curson et al., 2017; Williams et al., 2019). It is estimated that ~0.35 % of marine bacteria, mainly *Alphaproteobacteria*, contain *dsyB* (Curson et al., 2018), but *mmtN*, in some DMSP-producing *Alphaproteobacteria*, *Gammaproteobacteria* and *Actinobacteria*, is far less (~13-fold) abundant (Williams et al., 2019). Functional DsyB-like enzymes, termed DSYB exist in DMSP-producing eukaryotic algae (diatoms, haptophytes and dinoflagellates) and corals (Curson et al., 2018). The presence of *dysB*, *mmtN* and/or *DSYB* genes are robust reporters of microbial DMSP synthesis (Curson et al., 2017; Curson et al., 2018; Williams et al., 2019). A MTHB *S*-methyltransferase isoform enzyme, termed TpMMT, was identified and only ratified in the diatom *Thalassiosira pseudonana* (Curson et al., 2018; Kageyama et al., 2018).

When released into the environment, DMSP is imported by diverse marine bacteria and algae (Simó and Pedrós-Alió, 1999; Sun et al., 2011), which can use it for its anti-stress properties (Otte et al., 2004) or can catabolise it as a source of carbon, reduced sulfur and/or energy (Kellogg et al., 1972; Tripp et al., 2008; Curson et al., 2011). Bacteria modify DMSP by three known pathways - the demethylation pathway, the cleavage pathway and a oxygenation pathway generating dimethylsulfoxonium propionate (DMSOP) (Thume et al., 2018).

Most environmental DMSP (~75%) is thought to be transferred into the bacterial biomass via DMSP demethylation that can generate the reactive gas methanethiol (Kiene and Linn, 2000).

The first and key step of DMSP demethylation is catalysed by the bacterial DMSP demethylase encoded by *dmdA* (Howard et al., 2006), which is widely used as the reporter gene for DMSP demethylating bacteria (Varaljay et al., 2010). Previous metagenomic studies predict *dmdA* to be in ~60% of marine bacteria and widely distributed in marine environments (Howard et al., 2006; Howard et al., 2008). The *dmdA* gene is divided into five clades (clade A, B, C, D, E) and fourteen subclades (Varaljay et al., 2010), with subclades C/2 and D/1 being most abundant in marine samples (Varaljay et al., 2012; Cui et al., 2015b).

DMSP cleavage pathways are predicted to account for ~10% of DMSP catabolism (Kiene and Linn, 2000). Eight DMSP lyase enzymes are known to cleave DMSP generating the climate active gas dimethyl sulfide (DMS) and acrylate or 3-hydroxypropionate in taxonomically diverse bacteria and algae (Curson et al., 2011; Alcolombri et al., 2015; Sun et al., 2016; Bullock et al., 2017). The DMSP lyases including DddD, DddL, DddP, DddQ, DddW, DddY and DddK from bacteria and fungi (DddP) and Alma1 from algae belong to distinct protein families (Curson et al., 2011; Alcolombri et al., 2015; Johnston, 2015; Sun et al., 2016; Bullock et al., 2017). Of these genes, *dddP* is the most frequently detected *ddd* gene in marine metagenomes, predicted to be present in ~8% of marine bacteria (Todd et al., 2009; Raina et al., 2010; Peng et al., 2012; Curson et al., 2018). Being the most abundant DMSP lyase gene, *dddP* is widely used as a reporter of environmental DMSP cleavage (Liu et al., 2018; Sun et al., 2020).

Culture-dependent and -independent microbial studies have investigated how environmental factors impact the distribution and diversity of *dddP* and *dmdA* in varied marine environments (Cui et al., 2015a; Kuek et al., 2016; Zeng et al., 2016; Liu et al., 2018). Such studies found these two genes to be taxonomically diverse and widespread across almost all major oceans, from tropical waters to the polar sea (Peng et al., 2012; Zeng et al., 2016). In comparison to DMSP catabolism, there are few molecular studies on environmental DMSP production and

these showed bacterial DMSP production to be significant in surface coastal sediment, marine sediment and seawater, sea surface microlayer and deep ocean environments (Williams et al., 2019; Song et al., 2020; Sun et al., 2020; Zheng et al., 2020). No molecular genetic studies have investigated the changes in abundance and diversity of DMSP synthesis and catabolic potential across the salinity gradient of an estuary. This is important because many model bacteria and algae (Curson et al., 2017; Curson et al., 2018; Williams et al., 2019) are known to regulate DMSP production according to salinity and nutrient availability, properties that vary considerably in the gradients that exist along an estuary.

Large-river estuaries are important interfaces between continents and oceans. They are biogeochemical hotspots due to the large inputs of particulate matter, organic carbon and nutrients from both continents and oceans, thus supporting high rates of metabolic and chemical reactions (Zhai et al., 2017). The Changjiang River, also known as the Yangtze River, is the longest river in the Euro-Asia continent, which plays an important role in global biogeochemical cycling (Hou et al., 2008). Nutrients carried by the river are essential sources for phytoplankton primary production, which influence the bacterial community (Zhou et al., 2007), as does the hydrological characteristics, especially the salinity gradient in different seasons (Zheng et al., 2016).

Here we investigate microbial community and DMSP and DMS (in summer only) standing stock concentration changes associated with the transition from fresh to marine waters in the Changjiang Estuary and adjacent coastal areas in summer and winter. We also study the distribution and diversity of DMSP synthesis and catabolic (primarily *dddP* and *dmdA*) genes and the influence of environmental factors in different seasons and regions.

Results

Environmental parameters

Waters from 15 sites (Fig. 1) covering a transect from freshwater, through transition, to seawater, were sampled in winter and summer, and environmental parameters are summarized in Table S1 and S2. The primary productivity of the waters, reflected by Chl *a* levels, and water temperatures were generally lower in the winter than in the summer, especially for the transition and seawater region (Fig. S1, Table S1, S2 and S3). NH_4^+ levels were also higher in the summer (mean of 6.69 μM) than winter (mean of 3.07 μM) samples (Table S1, S2 and S3). Many key nutrients (SiO_3^{2-}, PO_4^{3-} and NO_3^-) generally decreased in concentration moving away from the coast in both seasons.

Chl *a* levels decreased with the increased distance from coast (i.e. with increased salinity and decreased key nutrient concentrations) in winter, suggesting that the highest winter primary production was in freshwater samples (Fig. S1 and Table S1). In contrast, the transition region showed highest mean Chl *a* concentration in the summer, and consequently DO levels (Fig. S1 and Table S2).

DMSP concentration correlated with salinity

The DMSP standing stock concentration within size-fractionated water samples were measured (Table S1 and Table S2). Total DMSP concentration was generally lower in winter (3.15, 7.81 and 6.26 nM for freshwater, transition and seawater regions) compared to summer samples (6.48, 21.86 and 14.92 nM for freshwater, transition and seawater regions) (Fig. 2). As expected, the Changjiang Estuary fresh water samples showed the lowest average $DMSP_t$ concentrations compared to those from transition and seawater regions in winter and summer. This is consistent with DMSP synthesis being upregulated by increased salinity in bacteria and algae

(Curson et al., 2017; Curson et al., 2018; Williams et al., 2019) and with it having a role as an osmoprotectant (Zhang et al., 2019). DMSP concentration increased abruptly reaching a maximum at the junction between transition and seawater regions, and then decreased (Fig. 2). Even though the freshwater samples had the lowest average DMSP stocks, their levels were still significant, being only 2.48 and 1.99-fold lower in winter, and 3.38 and 2.30-fold lower in summer, than those of transient and marine samples, respectively. In the winter samples DMSP concentration did not correlate to Chl *a*, likely due to the majority of phototrophs being present in the freshwater regions (Fig. 2 and Fig. S1). In the summer samples, Chl *a* levels were highest in the transition zone, but peaks in this indicator for primary production did not match well to spikes in DMSP concentration (Fig. 2 and Fig. S1).

DMSP was mainly found within microorganisms or attached to particulate, with 46.1%-70.6% (in winter) and 64.6%-75.4% (in summer) of the total DMSP being captured in this form ($DMSP_{p1}$ {>3 μm} and $DMSP_{p2}$ {0.22-3 μm}, Fig. 2). $DMSP_{p1}$ (considered to be in algae and particle-associated {PA} bacteria) accounted for 23.7%, 51.6% and 25.5% in winter and 36.1%, 54.0% and 57.0% in summer for freshwater, transition and seawater regions, respectively, implying the significant role of larger microorganisms in DMSP synthesis and/or storage, especially in the summer. However, the proportion of $DMSP_{p2}$ (in free-living {FL} bacterioplankton and picoeukaryotes) was not insignificant (Fig. 2), and in winter (19.0% and 31.6% of $DMSP_t$) was 1.21 and 4.14-fold higher for transition and seawater samples than in summer (15.7% and 7.6% of $DMSP_t$), implying that smaller microorganisms, e.g. bacteria, may also be important for DMSP production of the Changjiang Estuary, particularly in winter.

Dissolved DMSP stocks, those which are available for uptake and catabolism by microorganisms, are consistently low (0.16-5.54 nM) throughout the freshwater, transition and seawater samples in winter, despite $DMSP_t$ and $DMSP_p$ levels being much higher in transition samples (Fig. 2A, 2B and 2C). The situation is very different in summer samples, with the

lowest levels being observed in the freshwater samples (0.09-4.37 nM), that increase to the highest levels in the transient zone (1.88-18.41 nM) before decreasing to the seawater levels (0.94-18.51 nM) (Fig. 2D, 2E and 2F). Thus, DMSP availability in the summer mirrors that of $DMSP_t$ and $DMSP_p$, implying that more DMSP is available for catabolism in the summer transition zone.

The winter samples showed no obvious differences in DMSP stock concentration between surface and bottom waters. In contrast, the $DMSP_t$ concentration of surface water samples were higher than those from the bottom water in summer transition region (1.9-fold). However, it should be noted that all samples were taken in the photic zones, thus, one might not necessarily expect a large divide that might result, e.g. from a lack of phototrophs in the deeper samples.

The DMS concentration in summer samples, ranging from 0.71-8.62 nM, had a similar distribution pattern to DMSP. The peak DMS value was in the junction of transition (0.90-8.62 nM) and sea water regions (0.71-6.85 nM) (Fig. S2), and likely results from DMSP cleavage. Interestingly, the freshwater samples also had a considerable DMS levels, as with DMSP, in these summer samples, ranging from 1.77-5.63 nM. Summer DMS concentration was positively correlated with temperature, DO and Chl *a* ($P = 0.001$, 0.001 and 0.035, respectively), implying the close interrelation of DMS, DMSP and eukaryote algae. Unfortunately, we have no DMS data for the winter samples.

In the following sections we investigate the correlations between DMS, $DMSP_t$, $DMSP_{p1}$, $DMSP_{p2}$ and $DMSP_d$ concentrations in water samples and their microbial communities and genetic potential to both synthesise and catabolise DMSP.

Microbial community changes associated with salinity change

16S rRNA amplicon sequencing was carried out on all samples (Table S4) and 7305 OTUs were assigned at cut-off level of 97% nucleotide identity. Generally, PA bacteria exhibited

higher OTU diversity than FL bacteria especially in winter (mean of 1318 and 705 OTUs, respectively, Table S4). Furthermore, the OTU diversity of bottom water samples was slightly higher (1.1 to 1.5-fold) than in surface water, most notably in the PA fraction with 1075 and 772 OTUs for surface and 1562 and 1006 OTUs for bottom water in winter and summer, respectively (Table S4). The Shannon and Chao 1 index were used as proxies for evaluating bacterial community diversity and richness, respectively. There were significant differences in bacterial diversity and richness among regions and/or between seasons for PA and FL bacteria (Fig. S3 and S4).

It is generally thought that algae are the major producers of DMSP in photic marine environments. The prominence of eukaryotic plastid 16S rRNA genes and metagenomics were used to identify potentially key DMSP-producing algae in the samples. The dominant algae detected in the 16S rRNA data of all samples were Bacillariophyta (diatoms, 1.82% and 0.87% of 16S rRNA sequences for the PA fraction while 0.97% and 0.70% for FL in winter and summer, respectively) and Cryptomonadaceae (0.96% and 0.47% of 16S rRNA sequences for PA while 0.35% and 0.23% for FL in winter and summer, respectively) (Fig. S5). The majority of Cryptomonadaceae phytoplankton tested in (Keller et al., 1989) did not produce DMSP nor do they have DSYB (Curson et al., 2018) and diatoms are generally known as low producers of DMSP (typically < 50 mM intracellular) (Keller et al., 1989). Metagenomics analysis found algal DNA (total amount of reads affiliated to microalgae) to represent ~ 0.012% of the metagenome data (Fig. S6). Metagenomics data did not support the 16S rRNA data well with the *Pelagophyceae* class, not *Cryptomonadaceae* or *Bacillariophyta*, generally dominating (Fig. S6). *Pelagomonas* spp. have been shown to contain moderate intracellular DMSP levels (15.4-31.4 mM) (M. Corn, 1996), and express the *Alma1* DMSP lyase (Vorobev et al., 2020). DMSP producers such as *Emiliania* of *Prymnesiophyta*, *Ulvophyceae* and *Dinophyceae* genera were detected but at much lower levels in the metagenome data. Given the larger size of these phytoplankton, particularly diatoms, in comparison to bacteria, it is likely they significantly

contribute to the DMSP production in these samples. This is especially likely in the PA fractions where they constitute a higher proportion of the 16S rRNA data (~2.1-fold and 1.5-fold higher in winter and summer samples) than in the FL fractions irrespective of the season. However, it is noteworthy that there was no significant difference in algal DNA abundance between FL and PA fraction of metagenomic data (P = 0.337).

In the transitional summer samples with the highest DMSP levels, algae were ~2-fold more abundant than in the winter in the 16S rRNA data. However, this scenario was reversed for the seawater samples where diatoms were ~10-fold more abundant in the winter than in summer (Fig. S5). It should be noted that there is no strong correlation between diatom abundance and DMSP concentration in these samples, but diatom abundance was positively correlated with Chl *a* concentration in summer (P = 0.004 for FL and 0.006 for PA). Thus, although algae are likely important DMSP producers in these photic samples, heterotrophic organisms may also be important producers.

To evaluate the potential importance of bacteria in DMSP production and cycling in these samples, the relative abundance of genera that are reported to produce and/or catabolise DMSP were analysed from the 16S rRNA amplicon data (Fig. S7 and S8). Generally, *Alteromonas*, *Roseovarius*, *Thiobacimonas* (*Salipiger*) and *Marinobacter* were the major observed bacterial genera predicted to make DMSP, besides the *Nisaea* genus in winter samples (Fig. S7). There was no significant difference in the relative abundance of predicted DMSP-producing genera in freshwater samples between seasons (P = 0.088 for FL and 0.175 for PA). In contrast, the relative abundance of DMSP-producing bacterial genera was generally higher in summer than winter in transition (P = 0.004 and 0.002, 2.8-fold and 5.3-fold for FL and PA fraction, respectively) and the PA seawater regions (P = 0.003, 3.2-fold for PA fraction) (Fig. S7). This contradicts the DMSP data that found ~1.21-fold (transitional samples) and 4.15-fold (seawater samples) higher DMSP levels in the winter bacterioplankton fraction compared to the summer,

and is consistent with Williams et al (2019) that proposes there are still many DMSP-producing bacterial genera that remain unidentified (Williams et al., 2019). Unsurprisingly, predicted DMSP-producing bacteria were least abundant in freshwater samples, with 0.31% and 0.24% in winter, and 0.50% and 0.10% in summer of FL and PA bacteria, respectively, predicted to have this capacity. These predicted levels of bacterial DMSP producers climbed to 0.60% and 0.32% in winter, and 1.71% and 1.69% in summer for the transition region, and are also high in the seawater samples from the winter (0.60% and 0.53% for FL and PA bacteria) and summer (mean of 1.49% and 1.69% for FL and PA fraction) (Fig. S7).

Metagenomics analysis (Fig. S9) also predicted *Marinobacter* and *Roseovarius* to be major DMSP producing bacteria, but *Alteromonas* and *Thiobacimonas* (*Salipiger*) appeared less abundant than in the 16S rRNA amplicon analysis. *Marinobacter* was far more abundant in the tested winter metagenomes (different from 16S rRNA amplicon data which may due to the smaller sample size). In contrast, the relative abundance of *Roseibacterium*, *Roseovarius*, *Ruegeria* and *Rhodobacter* were significantly higher in summer samples than in winter (P = 0.004, 0.006, 0.004 and 0.004, respectively. Fig. S9).

Turning attention to DMSP catabolism, SAR11 (most abundant, 0-21.49%) and *Roseobacter* clade bacteria (0.01%-5.88%), both well known to demethylate and cleave DMSP (Curson et al., 2011; Sun et al., 2020), were very abundant in most samples, especially in winter (Fig. S8 and S10). There was no significant difference in the abundance of bacteria, principally SAR11, predicted to catabolise DMSP in the PA fraction of freshwater and transition regions, nor was there in freshwater of FL bacteria between seasons (P = 0.347, 0.191 and 0.834, respectively). However, the relative abundance of such FL DMSP consumers was higher in transition summer (5.49%) than in winter (2.76%) samples. Interestingly, the reverse was seen in the FL seawater samples (7.41% in summer and 13.2% in winter), a likely consequence of SAR11 bacteria being significantly more abundant in winter seawater than in the other two regions (P = 0.001,

Fig. S8). In summer samples, there was no noteworthy difference in SAR11 relative abundance between the three regions, which may be due to the violent mixing of freshwater and seawater, but there was a peak in freshwater for SAR11 in PA form (P = 0.888, Fig. S8). *Roseobacter* clade genera (*Nautella*, *Maribius*, *Sulfitobacter*, *Thalassobius*, *Shimia* and *Labrenzia* that account for 3.91% and 26.39% in summer of total DMSP consumers, and 0.88% and 0.56% in winter for FL and PA fraction, respectively) were higher in summer than in winter (Fig. S8), indicating their potential contribution to DMSP catabolism. These *Roseobacter* bacteria were most prominent in the transition and seawater regions where the dissolved DMSP concentration of both seasons were highest (Fig. 2 and Fig. S8).

Metagenomic data generally supports the 16S rRNA amplicon analysis, with SAR11 (*Pelagibacter*) and *Roseobacter* clade bacteria predicted to be the dominant DMSP consumers (Fig. S10). However, in contrast to the 16S rRNA amplicon data, metagenomics predicts there to be: more known DMSP consumers in FL than PA samples in both winter and summer; and greater diversity of known DMSP consumers in summer compared to winter samples. It seemed that SAR11 clade was dominant in winter samples and *Roseobacter* clade bacteria, e.g. *Roseobacter*, *Roseibacterium*, *Roseovarius* and *Loktanella* in summer samples (Fig. S10). The contrasting metagenome and 16S rRNA amplicon data may due to the smaller metagenomic sample size (Fig. S8 and S10).

The methods used here to predict the importance of DMSP producers and consumers are likely inaccurate, since they assume that all members of the same genera have these phenotypes (overestimating the importance). Furthermore, there are many unknown genera that can produce and/or catabolise DMSP (underestimating the importance) (Liu et al., 2018). Analysis of marker genes for the individual processes in metagenomes and by qPCR/RT-qPCR is likely a better indicator of their importance due to direct gene quantification in the samples.

Eukaryotic DMSP synthesis genes in samples

Metagenomics was carried out (Fig. 3) on representational FL and PA samples from transitional and marine sites taken in summer and winter that generally contained the highest DMSP stock concentrations. There were no detectable *TpMMT* genes within the metagenomic data which is surprising considering the 16S rRNA data implied that diatoms were the amongst the most abundant phytoplankton in the samples. In contrast, there were some algal *DSYB* sequences identified in 5 of 12 samples (mainly in FL fractions) comprising only 7 sequence reads (Fig. S11 and S12). These putative DSYB sequences, most similar to sequences from *Ochrophyta* and some green algae, were located in inshore sites, which may be due to the high nutrition concentrations in these regions (Fig. S12). Interestingly, the putative *DSYB* genes were far less abundant than the prokaryotic *dsyB* equivalents (Table S5), but because of the extremely low levels of algal DNA in the metagenomes (~0.012%) the percentage of algae predicted to contain DSYB in some samples was quite high (Fig. S11). Deeper metagenomics sequencing, to capture more of the larger eukaryotic genomic context, and metatranscriptomics and/or metaproteomics data would have been useful to better capture algal DMSP synthesis potential.

Prokaryotic DMSP synthesis genes in samples

To investigate the importance of bacterial DMSP production in our samples, qPCR was used to examine the abundance of the bacterial DMSP synthesis genes *dsyB* and *mmtN*. Although there were exceptions (e.g. WA6-3S and SA6-4B), the *dsyB* gene was more abundant in FL bacteria from winter and summer samples (~2.0-fold and 3.4-fold, respectively, Table 1) than PA bacteria (Fig. 4A and 4B). The fact that *dsyB* was detected in PA fraction signifies that fractionation is not an ideal methodology to distinguish bacteria from algae and their relative importance in processes, e.g. DMSP synthesis. Bacteria with *dsyB* were more abundant during

the summer rather than winter seasons in both freshwater (P = 0.014 and 0.009 for FL and PA) and seawater (P = 0.007 and 0.049 for FL and PA). There was more variability in *dsyB* abundance in the transition samples with the maximal levels being in higher salinity regions of the summer samples (from 5.11×10^0 and 1.26×10^0 copies ml^{-1} to 1.40×10^3 and 3.68×10^2 copies ml^{-1} for FL and PA fraction, respectively), but *dysB* distribution was more unified in the transition sites of winter samples (ranging from 9.00×10^{-1} to 6.91×10^2 copies ml^{-1}) (Fig. 4A and 4B). On average *dsyB* abundance (Table 1) and DMSP stocks (Fig. 2) were lowest in the freshwater samples (0.61-6.96×10^1 copies ml^{-1}) and were increased in the transitional (0.87-4.11×10^2 copies ml^{-1}) and seawater regions (0.62-8.60×10^2 copies ml^{-1}) with higher salinities in both summer and winter samples (Fig. 4, Table S6 and S7). This is again consistent with DMSP being an osmolyte produced as organisms encounter regions of increased salinity.

Consistent with previous work (Williams et al., 2019; Sun et al., 2020), bacteria with *mmtN* were less abundant (<60 copies ml^{-1} for most samples) than those with *dsyB* in all samples (Table 1, Fig. 4C and 4D). In winter samples *mmtN* abundance is lowest in freshwater samples (mean of 5.76×10^{-1} and 1.99×10^0 copies ml^{-1} for FL and PA bacteria, respectively) with higher levels detected in the transition and seawater samples (mean values with 2.99×10^0 to 3.07×10^1 copies ml^{-1}, Table 1, Fig. 4C). This is not the case in the summer samples where *mmtN* abundance is universally low (Fig. 4D).

Metagenomic data was also interrogated to predict the relative abundance of DsyB and MmtN in representational transitional and seawater samples. The *dsyB* gene was found in all samples with 0.63%-1.62% of bacteria in winter and 0.28%-1.45% in summer predicted to contain this gene (Fig. 3). The DsyB sequences were mostly homologous to *Roseobacter* clade bacteria such as *Roseovarius*, *Thalassobaculum*, *Albimonas* (Fig. S12). Consistent with qPCR analysis, the *mmtN* gene was far less abundant than *dsyB* in the tested transitional and marine samples (Fig. 3). *mmtN* was detected in 4 of 12 samples with a mean relative abundance of 0.19% and

the environmental MmtN sequences most closely aligned to *Roseovarius*, *Labrenzia* and *Rhodobacter* MmtN (Fig. S13). There was no significant difference in the relative abundance of *dsyB* (P = 0.423) and *mmtN* (P = 0.216) between the FL and PA metagenomes. This data contradicts the more sensitive qPCR experiments, above, and is likely a consequence of the limited sequencing in this study, but it does again highlight the message that fractionation does not effectively separate bacteria from algae.

RT-qPCR analysis was also carried out on freshwater, transitional and seawater samples to further predict the activity of DMSP-producing bacteria in our samples. *dsyB* transcripts were undetectable in freshwater samples, but were universally transcribed in all tested transitional (1.47-7.68 × 10^1 copies ml^{-1} in winter and 0.36-3.33 × 10^1 copies ml^{-1} in summer) and seawater samples (1.64-5.67 × 10^1 copies ml^{-1} in winter and 0.51-1.88 × 10^1 copies ml^{-1} in summer) at low levels (Fig. 5A, Table 2). This supports the hypothesis that bacteria are upregulating DMSP production in response to increased salinity with DMSP acting as an osmoprotectant. *dsyB* transcripts from FL bacteria in winter (5.44 × 10^1 copies ml^{-1}) were ~4.5-fold more abundant than in summer (1.20 × 10^1 copies ml^{-1}) (P = 0.006, Table 2, Fig. 5A), which could be explained by the higher salinity of transition water in winter (PSU 25.39) compared to the summer (PSU 21.99). There was no strong correlation between *dsyB* transcript level and DMSP concentration. Much like *dsyB*, *mmtN* gene transcripts were not detected in any freshwater samples but were found in 4 of 6 transitional and 3 of 6 seawater samples at very low levels (Fig. 5B). *mmtN* transcripts were always less abundant than those for *dsyB*, again confirming the likely dominance of the bacterial transamination pathway for DMSP synthesis over the methylation pathway, which is thought to be more important in sediment environments (Williams et al., 2019). *dsyB* and *mmtN* gene abundance and transcription levels, much like DMSP concentrations above, were not always higher in the marine versus the transition samples (Fig. 4, 5A and 5B), perhaps highlighting the greater need for DMSP under the stress of acclimating to higher salinity in the transition zone compared to the seawater zones where organisms may

365 already be acclimated.

366 To better understand the bacteria likely producing DMSP in our samples, clone libraries were
367 generated from FL *dsyB* qPCR products and 194 clones sequenced. The *dsyB* sequences
368 clustered into 23 OTUs (Fig. 6) with all having >80 % nucleotide identity to ratified *dsyB*
369 sequences. OTU1 and OTU2, homologous to *Donghicola sp*. and *Salipiger bermudensis*,
370 respectively (Fig. 6), were most abundant and may be important DMSP producing FL bacteria
371 in the Changjiang Estuary. Transition and seawater samples possessed a higher diversity of
372 *dsyB* than freshwater samples (Fig. 6). All OTUs were grouped into 8 clusters, and cluster 1,
373 which is not closely related to *dsyB* from any known bacterium, and cluster 2, closely related
374 to *Roseovarius indicus* and *Defluviimonas* sp. *dsyB*, showed the highest diversity (Fig. 6).

375 Cumulatively, qPCR and metagenomics work showed that the bacterial DMSP synthesis genes
376 *dsyB* and *mmtN* were far more abundant than their algal equivalents, *DSYB* and *TpMMT*; and
377 their bacterial transcripts were detected in most transitional and marine samples, indicating that
378 bacteria may be important contributors to DMSP production in these photic samples (Fig. 3).
379 Also, unlike other studies (Zhang et al., 2014a), Chl *a* (indicative of algae) showed no
380 significant correlation with $DMSP_t$ in winter (P = 0.078), but bacteria with *dsyB* gene had a
381 significant positive correlation with $DMSP_t$ (P = 0.011 and 0.042 for FL and PA bacteria,
382 respectively, Table S6 and S7). However, there was no such significant correlation for Chl *a* or
383 bacteria with *dsyB* (P = 0.582 and 0.175 for FL and PA fractions, respectively) to DMSP in the
384 summer samples.

385 **Abundance of DMSP-catabolic genes in eukaryotes and prokaryotes**

386 Transitional and marine metagenomic data, above, was also analysed for known DMSP
387 catabolic genes. No eukaryotic *Alma1* DMSP lyase sequences were found in the metagenome

388 data. In contrast the *dmdA* and *ddd* genes were very abundant in these samples leading to the
389 hypothesis that bacteria were the major DMSP catabolisers and were responsible for the bulk
390 of DMS detected in these waters (Fig. 3).

391 As the most abundant DMSP catabolic gene in seawater samples (Varaljay et al., 2010), the
392 abundance and transcription of *dmdA* was analysed by qPCR and RT-qPCR. *dmdA* was
393 significantly more abundant in FL than PA transitional and seawater dwelling bacteria in both
394 seasons (P = 0.003 and 0.009, ~1.9 and 8.0-fold in winter while ~5.3 and 4.9-fold in summer,
395 respectively, Table 1 and Fig. 7C and 7D). Indeed, *dmdA* transcripts follow the same trend in
396 seawater samples (~1.8 in winter and 2.3 in summer of the seawater samples, Table 2 and Fig.
397 5D) and winter transitional samples (~1.1-fold), but not in summer transitional samples where
398 *dmdA* transcripts is ~3.9-fold more abundant in the PA fractions (Fig. 5D). The abundance of
399 bacteria with *dmdA* and their *dmdA* transcripts was lowest in the freshwater samples [(0.75-
400 4.08) × 10^2 copies ml^{-1} for average] with the lowest $DMSP_d$ levels, and there was no significant
401 difference between FL and PA samples (P = 0.059, 0.294 for *dmdA* and P = 0.121, 0.439 for
402 *dmdA* transcripts in winter and summer, Fig. 5D, 7C and 7D). In both seasons, *dmdA* abundance
403 and DMSP concentration increased in the transitional [(0.09-2.52) × 10^4 copies ml^{-1} for average]
404 and seawater samples [(0.23-1.83) × 10^4 copies ml^{-1}] that had increased salinity and $DMSP_d$
405 (Fig. 7 and Fig. S1). A very similar trend was also seen for the *dmdA* transcripts (Fig. 5D, 7C
406 and 7D). *dmdA* abundance was significantly higher in summer (2.52 × 10^5 and 4.78 × 10^3
407 copies ml^{-1} for FL and PA bacteria, respectively) than in winter (1.68 × 10^3 and 8.98 × 10^2
408 copies ml^{-1} for FL and PA bacteria, respectively) for transitional water (P = 0.003 for FL
409 bacteria) but was at similar levels in freshwater and seawater regions between seasons (Fig. 7C,
410 7D and Table 1). Also, *dmdA* transcript levels were higher in summer than in winter seawater

411 samples (Fig. 5D and Table 2). In summer samples, the peak value of *dmdA* abundance was
412 located at the interface between transition and seawater (Fig. 7D).

413 Metagenomic analysis predicted DmdA to be in 3.24% - 4.96% and 1.98% - 16.83% of bacteria
414 of the winter and of summer samples, respectively (Fig. 3). There were no significant
415 differences between the relative abundance of *dmdA* between the seasons or the FL and PA
416 fractionation ($P = 0.200$, Fig. 3). The metagenomic DmdA sequences were mainly homologous
417 to *Pelagibacter* (SAR11 clade) and *Rhodobacteraceae* (e.g. *Roseobacter*, *Roseovarius*)
418 enzymes (Fig. S14).

419 As the most environmentally abundant DMSP lyase gene, *dddP* was also analysed by qPCR
420 and RT-qPCR. Bacteria with DddP and their *dddP* transcripts were least abundant in the
421 freshwater samples [means of $(0.67\text{-}2.94) \times 10^2$ and 0 copies ml^{-1}, respectively] with the lowest
422 DMSP levels. As expected, *dddP* levels increased with salinity in the transitional [means of
423 $(0.05\text{-}1.44) \times 10^4$ and $(0.46\text{-}1.58) \times 10^2$ copies ml^{-1}, respectively] and seawater samples [means
424 of $(0.04\text{-}1.63) \times 10^4$ and $(0.70\text{-}1.02) \times 10^2$ copies ml^{-1}, respectively] during both summer and
425 winter seasons where DMSP is more available (Fig. 5C, 7A, 7B, Table 1 and Table 2). However,
426 it was notable that there is no significant increase in DMS levels detected across all samples
427 irrespective of DMSP levels or *dddP* and its transcript abundance (Fig. 5C, 7A and 7B). As no
428 rate work was carried out in this study it is impossible to know the reason for this. *dddP* was
429 significantly more abundant in the FL fractions of seawater in both seasons ($P = 0.001$ and
430 0.001, ~5.2-fold in winter while ~28.4-fold in summer, respectively, Table 1 and Fig. 7A and
431 7B) and the summer transition samples ($P = 0.039$, ~3.9-fold, Table 1 and Fig. 7A and 7B)
432 compared to the PA fraction. However, there were exceptions in both the summer and winter

samples (notably, WA6-1B and -2B in winter, and SA6-2B, -3S, -4S and -3B in summer) where *dddP* was more abundant in PA fractions (Fig. 7A, 7B and Table 1). Within the transitional and seawater (FL only) samples with the highest DMSP levels, bacteria with *dddP* were significantly more abundant (P = 0.010 and 0.087, ~6.7 and 20.0-fold for FL and PA bacteria in transitional; P = 0.001, ~7.8-fold for FL bacteria in seawater) in summer than in winter (Fig. 7A, 7B and Table 1).

Interestingly, metagenomics analysis shows that *dddP* is significantly more abundant than *dmdA* in all tested samples (P = 0.001, Fig. 3). *dddP* is predicted to be present in 7.55% to 18.13% and 9.74% to 20.35% of bacteria in the winter and summer samples. It was slightly more abundant in tested summer (13.50% and 18.32% for FL and PA bacteria) compared to winter (10.43% and 14.32% for FL and PA fraction) samples, which was consistent with qPCR assay (Fig. 3, Fig. 7A and 7B). Furthermore, *dddP* was the most abundant DMSP lyase genes in the tested samples, being ~3.7-fold higher than *dddQ*, the second most abundant *ddd* gene (Fig. 3). These *dddP* sequences were closely related to *dddP* genes from *Rhodobacteraceae* (e.g. *Roseovarius* and *Ruegeria*) as well as some *Alphaproteobacteria* (e.g. *Rhodobacterales*) and Fungi (e.g. *Fusarium*) (Fig. S15). Given their clustering with functionally ratified DddP proteins, these environmental DddP sequences are expected to be functional DMSP lyase enzymes (Fig. S15).

After DddP, the next most abundant DMSP lyase detected in our metagenomes was *dddQ*, found in all samples and predicted to be in 2.07% to 5.43% and 2.39% to 8.84% of bacteria in the winter and summer samples, respectively (Fig. 3). There was no obvious difference between the abundance of *dddQ* in the winter and summer samples (Fig. 3). These *dddQ* sequences most

455 closely aligned to DddQ from *Rhodobacteraceae* (e.g. *Roseovarius* and *Ruegeria*) and
456 *Pelagibacteraceae* (Fig. S16) as well as other *Alphaproteobacteria* (e.g. *Rhodospirillaceae*,
457 *Rhizobiales*). *dddL* was the third most abundant DMSP lyase gene, again present in all
458 metagenome samples, and predicted to be in 0.28% to1.02% and 0.80% to7.60% of bacteria in
459 winter and summer samples, respectively (Fig. 3). *dddL* appeared to be more abundant in the
460 summer (1.33% and 3.45% for FL and PA, respectively) than in winter samples (0.41% and
461 0.76% for FL and PA fraction, respectively). The DddL sequences were most homologous to
462 *Rhodobacteraceae* (e.g. *Oceanicola*, *Rhodobacter* and *Labrenzia*) (Fig. S17) and other
463 Proteobacterial DddL enzymes, including, *Rhodospirillaceae* and *Marinobacter*. The SAR11
464 DMSP lyase gene *dddK* was detected in 9 of 12 samples and was predicted to be in 0.06% to
465 1.43% of bacteria (Fig. 3), which represents ~11.34% of the SAR11 detected (Fig. S18).

466 The *dddD* gene was detected in 4 of 12 metagenomic samples, and was predicted to be in 0.14%
467 to 0.63% of bacteria (Fig. 3). Some of these putative DddD sequences were closely related to
468 the functional enzymes (Fig. S19) and others were more closely related to DddD-like enzymes
469 in *Rhodobacteraceae* (e.g. *Ruegeria pomeroyii*) that do not have DMSP lyase activity and their
470 function unknown (Todd et al., 2011). Only one *dddW* sequence was found in summer sample
471 SA6-3 of PA fraction and this was homologous to a putative *Rhodobacteraceae* DddW from
472 *Sagittula* (Fig. 3). No *dddY* was found in this study, consistent with this enzyme being more
473 abundant in sediment environments. It is clear in these tested samples that cumulatively the
474 DMSP lyase genes are far more abundant than *dmdA* of the demethylation pathway, widely
475 thought to be the most abundant DMSP catabolic gene in marine samples (Varaljay et al., 2010).
476 Further work involving metatranscriptomics, metaproteomics, but most importantly detailed
477 process measurements of DMSP lysis and demethylation are required to support our hypothesis

that the DMSP cleavage pathway may be more important in the Changjiang Estuary than DMSP demethylation.

Discussion

Recent molecular studies of environmental DMSP synthesis have suggested that bacteria have a significant role in DMSP production and cycling in marine surface waters (Liu et al., 2018; Sun et al., 2020) and sediments (Williams et al., 2019), and non-photic environments e.g. the deep ocean (Zheng et al., 2020) and hydrothermal sediments (Song et al., 2020), that had been previously ignored. Until now, no molecular studies had investigated DMSP production and cycling in estuarine environments. However, many studies have investigated DMSP catabolism via the analysis of microbial communities and their catabolic gene abundance, distribution and transcription in diverse marine samples (Howard et al., 2008; Levine et al., 2012; Kudo et al., 2018; Liu et al., 2018), including some focused on estuarine regions (Williams et al., 2019; Han et al., 2020).

This molecular study of the Changjiang Estuary found the transition and seawater samples possessed higher DMSP and DMS levels and potential for bacterial DMSP production and catabolism and that this potential was more prominent in summer than winter seasons. It should be noted that this and most other published works on molecular DMSP/DMS cycling only consider the stocks of these compounds DMSP and these do not convey the flux through the relevant pathways. Furthermore, in such studies there also limitations due to the unavoidable time of sampling and filtration etc. in which rapid degradation of volatile organic sulfur compounds may occur (Wilkening et al., 2019).

Little evidence for algal DMSP production and cycling in the Changjiang Estuary

Algae, particularly haptophytes and dinoflagellates that can produce high intracellular levels of DMSP (10^2-10^3 mM) (Keller et al., 1989; Stefels, 2000), are largely thought to be responsible for the bulk of environmental DMSP in photic marine samples. However, in our tested estuary samples the only obvious link between algae and the observed DMSP levels was that the vast majority (23.7%-57%) of DMSP was found in the larger >3 μm PA fraction, which is most likely to contain algae. Note, metagenomics, qPCR and RT-qPCR showed that there can be significant levels of bacteria with the potential to produce DMSP and their *dsyB* and *mmtN* transcripts in the PA fractions. There was no correlation between DMSP levels and Chl *a*; observed algae in 16S rRNA data were previously shown not to produce DMSP (Keller et al., 1989) or be low producers in the case of diatoms (Curson et al., 2018); and finally, there were few detected *DSYB* and *Alma1*, and no *TpMMT* genes in the selected metagenomic data from transitional and seawater sites with the highest DMSP levels. It is likely that the metagenomic depth used in this study was insufficient to capture algal DMSP synthesis and catabolic potential, given their larger genome size and perhaps a meta-transcriptomic or -proteomic approach may have been more revealing. Thus, the data presented here does neither confirm or refute the importance of algal DMSP production and cycling in the Changjiang Estuary samples but it does however imply that bacteria could be significant DMSP-producers in the transition and seawater samples, and that they are most likely very significant DMSP catabolisers, see below.

Bacterial DMSP production and catabolism enrichment in transition and seawater regions

Unsurprisingly, this study showed freshwater, irrespective of seasonality, to possess the lowest DMSP levels, with the lowest proportion of bacteria capable of producing (with *dsyB* and *mmtN*) and catabolising (with *dddP* and *dmdA*) DMSP, and the lowest detected transcript levels for known DMSP cycling genes. Indeed, the highest levels of DMSP, predicted DMSP-producing and -catabolic bacteria and of their transcripts (*dsyB, mmtN dmdA* and *dddP*) were always found in the transitional and seawater regions of the Changjiang Estuary with increased salinities, irrespective of seasonality. This is consistent with: DMSP being produced as an osmoprotectant in marine environments (Zhang et al., 2019); DMSP levels and bacterial DMSP synthesis being upregulated by salinity (Williams et al., 2019); and bacteria with the potential to catabolise DMSP being found in environments with higher levels of their growth substrate (Curson et al., 2011). It is also consistent with Han et al. (2019) who found *dmdA* to be more prominent in in costal rather than less saline estuary samples from the Gwangyang bay in Korea Peninsula all year (Han et al., 2020). *Alteromonas*, *Roseovarius*, *Thiobacimonas* and *Marinobacter* bacteria, predicted to make DMSP and be more abundant in the transition and seawater than the freshwater region, were likely important DMSP producers in the Estuary samples (Fig. S7). For DMSP catabolism, *Roseobacter* clade bacteria (generally containing a *ddd* variant and *dmdA*), mainly located in transition and seawater region, and SAR11 in seawater, showed good correlation with $DMSP_d$ levels (Fig. 2 and Fig. S8) and were likely important DMSP degraders in the Changjiang Estuary.

Bacterial DMSP production and catabolic potential was higher in the summer

The distribution of bacterial DMSP producers, e.g. *Thiobacimonas* and *Marinobacter* (Fig. S7), and their known DMSP synthesis genes and transcripts (Fig. 4A, 4B and 5A) was consistent with increasing DMSP concentration and salinity (Fig. 2 and Fig. S1), which were all generally highest in the summer transitional and seawater samples than winter. This implies that bacterial DMSP production potential in the Changjiang Estuary is higher during the summer than in the winter. Given, *mmtN* was >7.0-fold less abundant than *dsyB*, and that *mmtN* transcripts were also less abundant, we propose the transamination pathway as the dominant aquatic bacterial DMSP synthesis pathway, and this is consistent with the findings of Williams et al. (2019) and Sun et al. (2020) (Williams et al., 2019; Sun et al., 2020). The caveat to this is that there are other unknown *S*-methyltransferase enzymes of DMSP synthesis pathways in bacteria and algae, e.g. in *Marinobacter* and *Crypthecodinium* (Uchida et al., 1996), that could not be considered here.

The relative abundance of DMSP consumers (e.g. *Nautella*, *Maribius*, *Sulfitobacter*, *Thalassobius*, *Shimia* and *Labrenzia*, Fig. S8) and their genes (*dddP* and *dmdA*, Fig. 3 and Fig. 7) in the transition region was higher in summer than in winter, which was consistent with the $DMSP_d$ concentrations (Fig. 2). These results were also consistent with Kudo et al. (2018), who found *dddP* to be more abundant in summer compared to winter samples from Ofunato Bay (Kudo et al., 2018). *dmdA* seawater transcripts and *dddP* transitional transcripts (PA) were also higher in summer samples than in winter (Fig. 5C and 5D). Furthermore, metagenomics showed *dddL* and *dddK* genes to be more abundant in summer compared to winter samples (Fig. 3). Overall, these results suggested that bacterial DMSP production and catabolic

potential was higher in the summer than in winter.

Bacterial DMSP production may be more important in winter than summer of the Changjiang Estuary

Even though DMSP levels and the abundance of bacteria with the potential to produce DMSP were generally greater in the summer than winter samples, the percentage of $DMSP_t$ in the 0.22-3μm fractions, apportioned to bacterioplankton, was higher in the winter transition and seawater samples (19.0% and 31.6% in winter; 15.7% and 7.6% in summer). It should be noted that due to rapid degradation of volatile organic sulfur compounds DMSP/DMS, it is important to minimize time between sampling in remote field locations and laboratory analysis (Wilkening et al., 2019). Furthermore, the proportion of plastid sequences to 16S rRNA data was lower in winter transition compared to the summer samples (Fig. S5), implying a reduced algal component in the winter samples. Thus, we hypothesise that bacteria may have a greater contribution to DMSPt levels in the winter when algae were less abundant. Further experiments are required to test this hypothesis in the Changjiang Estuary and other estuarine ecosystems.

Conclusions

This study highlights the transition and seawater regions of the Changjiang Estuary as hubs for the highest DMSP levels and bacterial DMSP synthesis and catabolic potential in both summer than winter samples. Algae are likely important DMSP producers in these transition and seawater regions but Chl *a*, metagenomics and 16S rRNA amplicon sequencing data do not support this hypothesis. Our data does support free-living bacteria as being important DMSP producers and consumers within the transition and seawater estuary samples. Changjiang Estuary bacterial DMSP production and cycling may be more prominent in summer, but bacterial DMSP synthesis likely contributes more to $DMSP_t$ levels in the winter when algae were likely less abundant. Overall, this study revealed the spatiotemporal distribution pattern

of DMSP production and catabolic genes and their transcript levels in the Changjiang Estuary. It provides an exemplar study for future estuarine research on microbial DMSP cycling.

Experimental Procedures

Sampling and environmental parameters

1 litre triplicate samples of surface (~1 m deep, the sample name ends with "S") and bottom (from 4 m to 62 m deep, the sample name ends with "B") water were collected aboard the R/V Runjiang I from 15 sites of the Changjiang Estuary in winter (February 2017, the sample name starts with "W") and summer (July 2017, the sample name starts with "S") using a Sealogger CTD (SBE25, Electronic Inc., USA) rosette water sampler (Fig. 1A). Here, we divided the Changjiang Estuary into three regions, the freshwater region (salinities < 1 PSU), transition region (1-30 PSU) and seawater region (salinities ≥ 30 PSU) according to (Liu et al., 2015). Four sites were in fresh water regions (C1, C3, C5 and C7 sites for surface and bottom water of winter and summer) whereas eleven sites were in transition areas (A6-1 to A6-4 sites for surface and bottom water in winter; A6-1 to A6-8 sites for surface water and A6-1 to A6-3 sites for bottom water in summer) and seawater regions (A6-5 to A6-11 for surface and bottom water in winter; A6-9 to A6-11 for surface water and A6-4 to A6-11 for bottom water in summer) (Fig. 1B and 1C). The samples were reordered by increasing of salinity regardless of the sampling depth to study the influence of salinity in the following analysis. One litre of seawater was pre-filtered through 3 μm polycarbonate membranes (Millipore Corporation, Billerica, MA, USA) to obtain PA bacteria, and then FL bacteria were collected using 0.22 μm polycarbonate membranes (Millipore Corporation, Billerica, MA, USA). Membranes were frozen in liquid nitrogen immediately, and then stored at -20℃ on board ship before transfer to -80℃ in the laboratory.

In situ hydrological parameters (temperature, salinity and depth) were monitored by CTD equipped on the water sampler. Chlorophyll *a* (Chl *a*) concentrations were measured essentially as Zhang et al. (2014) (Zhang et al., 2014b). Seawater was collected on 0.7 μm pore size GF5F filters (Whatman), and then Chl *a* was extracted with 90% (v/v) acetone for 24 h in the dark. The Chl *a* concentration was determined using a Turner-Designs Trilogy Laboratory® Fluorometer. DO was measured by Winkler method (Carpenter, 1965). Waters were filtered with 0.45 μm cellulose acetate membranes, and nutrients including PO_4^{3-}, NO_2^-, NO_3^-, SiO_3^{2-} and NH_4^+ were analyzed by a nutrient auto-analyzer (AA3, Seal Analytical Ltd, UK) (Liu et al., 2015). Enumeration of bacteria was estimated by the copy numbers of 16S rRNA genes which were quantified using qPCR.

DNA/RNA extraction and qPCR/RT-qPCR

Total DNA were extracted from 3 μm and 0.22 μm membranes using the Phenol-chloroform method (Sun et al., 2020). The extracted DNA was dissolved in 50 μl TE buffer (100 mM Tris-HCl, 10 mM EDTA, pH 8.0) and stored at -80℃ for further use. RNA was also extracted from 3 μm and 0.22 μm membranes as in the previous study (Liu et al., 2019), and reverse transcription of RNA was performed as Williams et al. (2019) with some modifications (Williams et al., 2019). Absence of DNA in RNA samples was confirmed by PCR using primers 338F/518R (Table 3), and 9 μl RNA were mixed with 1 μl 10 μM random reverse primer for the RNA reverse transcription. Finally, resultant cDNA was stored at - 80°C until use.

qPCR and RT-qPCR were performed using primers to the 16S rRNA gene, the DMSP biosynthesis genes *dsyB* and *mmtN* and catabolic genes *dddP* and *dmdA* (C/2, D/1 subclade). All primers and their annealing temperatures are shown in Table 3. The PCR reactions and melt curves were conducted as previous described in (Sun et al., 2020). qPCR standard curves were made using pUCm-T vector (Biotech, China) containing a single copy of the corresponding gene. Plasmids were extracted using Mini Plasmid Kits (TaKaRa, Tokyo, Japan), then

linearized by digestion with *Xho*I, purified by TIANgel Mini Purification Kit (TIANGEN Biotech, Beijing), and the concentrations of the products were quantified with a Nanodrop-1000 Spectrophotometer. The 10-fold serially diluted linearized plasmids were then used to generate standard curves with all liner correlations showing $R^2 > 0.99$. The amplification efficiencies were between 95% and 105% (*dsyB* and *mmtN* with 83% to 96%). Three technical replicates were set for each sample. All samples were run on StepOne™ Real-time PCR System (Applied Biosystems) and the acquired data were analyzed by StepOne software (version 2.2).

Clone library of *dsyB* gene and phylogenetic analysis

To sequence the *dsyB* amplicons from qPCR products above, *dysB* clone libraries were constructed from 21 samples of FL fractions (WA6-2S, WA6-2B, WA6-3B, WA6-6S, WA6-6B, WA6-7B, WA6-8B, WA6-11S, SC1B, SC3S, SA6-1S, SA6-3B, SA6-7S, SA6-8B, SA6-9S, SA6-9B, SA6-10S and SA6-11B). All PCR products were separated by electrophoresis in 1% agarose gels and then purified using a DNA gel extraction kit (Biomed, China). The purified *dsyB* gene amplicons were ligated into the pUCm-T vector (Sangon, China) and transformed into *Escherichia coli* JM109. Transformants with correct inserts detected by PCR were then sent for sequencing at the Sangon Biotech (Shanghai, China). The OTUs of *dsyB* were determined with nucleotide similarity of 80% by Mothur. Representative sequences of each OTU and other *dsyB* sequences were used to construct neighbor-joining phylogenetic trees using MEGA7 (Curson et al., 2017). The partial sequences of the *dsyB* gene from clone libraries are available in the GenBank database with accession numbers MZ297611-MZ297802.

The DMS and DMSP concentration measurements

In situ, DMS concentrations were measured by Gui-peng Yang's group but only for the summer samples (Yang et al., 2011). For the measurement of DMSP concentration, a gravity-filtration

658 method was applied to separate the different DMSP fractions. There are 4 DMSP fractions
659 examined, $DMSP_t$ (total DMSP in samples without filtration), $DMSP_{p1}$ (DMSP captured on 3
660 μm membrane, considered to contain algae and PA bacteria), $DMSP_{p2}$ (DMSP prefiltered
661 through a 3 μm membrane, captured on a 0.22 μm filter, considered to be mostly
662 picoeukaryotes and/or free-living bacteria) and $DMSP_d$ (dissolved DMSP present in filtrate that
663 filtered through 0.22 μm membrane, considered as cell-free DMSP available for the microbial
664 community to take up and/or catabolise). All the water samples for DMSP measurement were
665 stored in 4℃ with 0.5% H_2SO_4. Two milliliters of seawater samples were transferred into a
666 brown glass vial which contained 300 μl 10 M KOH solution, covered with a PTFE stopper
667 immediately and then sealed with an aluminum lid. Samples were incubated for at least 24 h in
668 the dark. DMS derived from the alkaline lysis of DMSP was assayed by cryogenic purge-and-
669 trap gas chromatography (Tan et al., 2017) on an Agilent GC-7890B machine.

670 **Bacteria community structure analysis**

671 The 16S rRNA gene of bacteria and plastids were amplified using primers 515modF and
672 806modR (Walters et al., 2016). The PCR reaction (20 μl) contained 1 × Fast Pfu Buffer, 0.25
673 mM of dNTPs, 0.2 μM of each primer, 1U of FastPfu Polymerase, 10 ng of template DNA, and
674 0.2 μl of BSA (bovine serum albumin). PCR cycling conditions were as follows: 35 cycles of
675 30 s at 95 °C, 30 s for annealing at 55 °C, and 45 s for elongation at 72 °C. Amplified PCR
676 products were purified using the AxyPrep DNA Gel Extraction Kit (Axygen Biosciences,
677 Union City, CA, USA) and quantified using QuantiFluor™-ST (Promega, USA) according to
678 the manufacturer's instruction. Purified amplicons were paired-end sequenced (2 × 300 bp) on
679 Illumina MiSeq platform (Illumina, San Diego, USA) according to the standard protocols by
680 Majorbio Bio-Pharm Technology Co. Ltd. (Shanghai, China). The raw reads were deposited
681 into the NCBI Sequence Read Archive (SRA) database (Accession Number: SRP174876).

682 After subsampling each sample to an equal sequencing depth (minimum number of sample

sequences with 25006 for each sample), operational taxonomic units (OTUs) were clustered with 97% similarity cutoff using QIIME1.9.1 by usearch7.0 method. The taxonomic position of representative 16S rRNA gene sequence for each OTU was analyzed by RDP Classifier (http://rdp.cme.msu.edu/) against the RDP 11.5 (to obtain eukaryotic plastid 16S rRNA sequences) and Silva 132 16S rRNA database using confidence threshold of 70%. The abundance of genera containing DMSP producing or catabolism genes were calculated according to the relative abundance of genera and bacterial absolute abundance (indicated by gene copies of qPCR).

Metagenome sequencing and analysis

DNA for metagenomic sequencing was extracted from 12 samples (WA6-2S, WA6S-2B, WA6-6B, SA6-2S, SA6-2B and SA6-6S from PA bacteria; WA6-2S, WA6-2B, WA6-6S, SA6-2S, SA6-2B and SA6-6S from FL bacteria) using NucleoSpin® Soil Kit (Macherey-Nagel, Düren, Germany). The DNA samples were sent to BGI (BGI, Shenzhen, China) company for metagenome sequencing. Metagenome assembly, taxonomic assignment and functional characterization were performed as in Liu et al. (2019) (Liu et al., 2019). BLAST analysis was performed to identify homologs of DMSP synthesis (*DSYB*, *TpMMT*, *dsyB* and *mmtN*) and catabolic genes (*Alma1*, *ddd*$^{+}$ and *dmdA*) in the samples as described in (Song et al., 2020). The frequency of these prokaryote and eukaryote genes was normalised to the number of *recA* and *β*-Actin sequences, giving the relative abundance as a percentage (Curson et al., 2017). Reference *recA* sequences were obtained from FunGene database (http://fungene.cme.msu.edu/), *β*-Actin from SwissProt database, *DSYB* from Curson et al 2018 (Curson et al., 2018) and other DMSP synthesis and catabolic genes/proteins are listed in Table S8. *dddD*, *dddL*, *dddQ*, *dddW*, *dddY* and *dddK* were referring to (Song et al., 2020). Sequences

obtained metagenomic analysis were used to construct neighbor-joining phylogenetic trees using MEGA7 (Curson et al., 2018). The metagenome data has been deposited in the NCBI Sequence Read Archive under accession numbers PRJNA732822.

Statistical analysis

Correlation analyses was conducted to identify links between the different environmental factors, bacterial genera and the abundance of functional genes using the Spearman correlation tests. Differences in environmental factors and gene abundance between seasons and sampling areas were conducted using the Mann-Whitney tests and Kruskal-Wallis tests. Statistical analysis was performed by SPSS version 25.0 (SPSS Inc., Chicago, IL, USA) and the significant threshold for all tests was set with $P < 0.05$ and $P < 0.01$. Alpha diversity indices including Chao1 and Shannon were performed by Mothur to estimate the richness and diversity of the bacterial communities.

Acknowledgements

We appreciate all the scientists and crew members on the R/V Runjiang I during the expedition for their great efforts and help in sample collection. We also thank Gui-Peng Yang of Ocean University of China for providing pH, DMS data and facilities for Chl *a* measurement, Weidong Zhai of Shandong University for providing DO data and Lijun Hou of East China Normal University for providing nutrient data. This work was financially supported by the National Key Research and Development Program of China (2016YFA0601303) and the National Natural Science Foundation of China (91751202 and 41730530) in X-HZ's laboratory. The Natural Environment Research Council UK Standard grants (NE/P012671 and NE/S001352) supported the work in JDT's laboratory.

Originality-Significance Statement

The authors confirm that the content of the manuscript is original, and the manuscript has neither been published previously, nor is being considered for publication elsewhere.

Conflicts of Interest

The authors declare no competing interests.

References

Ackman, R.G., Tocher, C.S., and McLachlan, J. (1966) Occurrence of dimethyl-β-propiothetin in marine phytoplankton. *Journal of the Fisheries Research Board of Canada* **23**: 357-364.

Alcolombri, U., Ben-Dor, S., Feldmesser, E., Levin, Y., Tawfik, D.S., and Vardi, A. (2015) Identification of the algal dimethyl sulfide-releasing enzyme: A missing link in the marine sulfur cycle. *Science* **348**: 1466-1469.

Bullock, H.A., Luo, H., and Whitman, W.B. (2017) Evolution of dimethylsulfoniopropionate metabolism in marine phytoplankton and bacteria. *Front Microbiol* **8**: 637.

Carpenter, J.H. (1965) The accuracy of the Winkler method for dissolved oxygen analysis. *Limnol Oceanogr* **10**: 135-140.

Cui, Y., Suzuki, S., Omori, Y., Wong, S.K., Ijichi, M., Kaneko, R. et al. (2015a) Abundance and distribution of dimethylsulfoniopropionate degradation genes and the corresponding bacterial community structure at dimethyl sulfide hot spots in the tropical and subtropical pacific ocean. *Appl Environ Microbiol* **81**: 4184-4194.

Cui, Y., Suzuki, S., Omori, Y., Wong, S.K., Ijichi, M., Kaneko, R. et al. (2015b) Abundance and distribution of dimethylsulfoniopropionate degradation genes and the corresponding bacterial community structure at dimethyl sulfide hot spots in the tropical and subtropical pacific ocean. *Appl Environ Microbiol* **81**: 4184-4194.

Curson, A.R., Todd, J.D., Sullivan, M.J., and Johnston, A.W. (2011) Catabolism of dimethylsulphoniopropionate: microorganisms, enzymes and genes. *Nat Rev Microbiol* **9**: 849-859.

Curson, A.R., Liu, J., Bermejo Martinez, A., Green, R.T., Chan, Y., Carrion, O. et al. (2017) Dimethylsulfoniopropionate biosynthesis in marine bacteria and identification of the key gene in this process. *Nat Microbiol* **2**: 17009.

Curson, A.R.J., Williams, B.T., Pinchbeck, B.J., Sims, L.P., Martinez, A.B., Rivera, P.P.L. et al. (2018) DSYB catalyses the key step of dimethylsulfoniopropionate biosynthesis in many phytoplankton. *Nat Microbiol* **3**: 430-439.

760 Dickson, D.M., Jones, R.G., and Davenport, J. (1980) Steady state osmotic adaptation in Ulva
761 lactuca. *Planta* **150**: 158-165.

762 Gage, D.A., Rhodes, D., Nolte, K.D., Hicks, W.A., Leustek, T., Cooper, A.J., and Hanson, A.D.
763 (1997) A new route for synthesis of dimethylsulphoniopropionate in marine algae. *Nature* **387**:
764 891-894.

765 Han, D., Kang, H.Y., Kang, C.K., Unno, T., and Hur, H.G. (2020) Seasonal mixing-driven
766 system in estuarine-coastal zone triggers an ecological shift in bacterial assemblages involved
767 in phytoplankton-derived DMSP degradation. *Microb Ecol* **79**: 12-20.

768 Hou, L.J., Liu, M., Ou, D.N., Yang, Y., and Xu, S.Y. (2008) Influences of the macrophyte
769 (Scirpus mariqueter) on phosphorous geochemical properties in the intertidal marsh of the
770 Yangtze Estuary. *J Geophys Res-Biogeo* **113**.

771 Howard, E.C., Sun, S., Biers, E.J., and Moran, M.A. (2008) Abundant and diverse bacteria
772 involved in DMSP degradation in marine surface waters. *Environ Microbiol* **10**: 2397-2410.

773 Howard, E.C., Henriksen, J.R., Buchan, A., Reisch, C.R., Burgmann, H., Welsh, R. et al. (2006)
774 Bacterial taxa that limit sulfur flux from the ocean. *Science* **314**: 649-652.

775 Johnston, A.W. (2015) Who can cleave DMSP? *Science* **348**: 1430-1431.

776 Kageyama, H., Tanaka, Y., Shibata, A., Waditee-Sirisattha, R., and Takabe, T. (2018)
777 Dimethylsulfoniopropionate biosynthesis in a diatom Thalassiosira pseudonana: Identification
778 of a gene encoding MTHB-methyltransferase. *Arch Biochem Biophys* **645**: 100-106.

779 Keller, M., Bellows, W., and Guillard, R. (1989) Dimethyl sulfide production in marine
780 phytoplankton. In *American Chemical Society (Symposium Series 393)*, pp. 167-182.

781 Kellogg, W.W., Cadle, R.D., Allen, E.R., Lazrus, A.L., and Martell, E.A. (1972) The sulfur
782 cycle. *Science* **175**: 587-596.

783 Kiene, R.P., and Linn, L.J. (2000) The fate of dissolved dimethylsulfoniopropionate (DMSP)
784 in seawater: tracer studies using 35S-DMSP. *Geochim Cosmochim Acta* **64**: 2797-2810.

785 Kocsis, M.G., and Hanson, A.D. (2000) Biochemical evidence for two novel enzymes in the
786 biosynthesis of 3-dimethylsulfoniopropionate in Spartina alterniflora. *Plant Physiol* **123**: 1153-
787 1161.

788 Ksionzek, K.B., Lechtenfeld, O.J., McCallister, S.L., Schmitt-Kopplin, P., Geuer, J.K., Geibert,
789 W., and Koch, B.P. (2016) Dissolved organic sulfur in the ocean: Biogeochemistry of a
790 petagram inventory. *Science* **354**: 456-459.

791 Kudo, T., Kobiyama, A., Rashid, J., Reza, M.S., Yamada, Y., Ikeda, Y. et al. (2018) Seasonal
792 changes in the abundance of bacterial genes related to dimethylsulfoniopropionate catabolism
793 in seawater from Ofunato Bay revealed by metagenomic analysis. *Gene* **665**: 174-184.

794 Kuek, F.W.I., Mujahid, A., Lim, P.T., Leaw, C.P., and Muller, M. (2016) Diversity and dMS(P)-
795 related genes in culturable bacterial communities in Malaysian coastal waters. *Sains*
796 *Malaysiana* **45**: 915-931.

797 Levine, N.M., Varaljay, V.A., Toole, D.A., Dacey, J.W., Doney, S.C., and Moran, M.A. (2012)

798 Environmental, biochemical and genetic drivers of DMSP degradation and DMS production in
799 the Sargasso Sea. *Environ Microbiol* **14**: 1210-1223.

800 Liu, J., Fu, B., Yang, H., Zhao, M., He, B., and Zhang, X.H. (2015) Phylogenetic shifts of
801 bacterioplankton community composition along the Pearl Estuary: the potential impact of
802 hypoxia and nutrients. *Front Microbiol* **6**: 64.

803 Liu, J., Liu, J., Zhang, S.H., Liang, J., Lin, H., Song, D. et al. (2018) Novel insights into
804 bacterial dimethylsulfoniopropionate catabolism in the East China Sea. *Front Microbiol* **9**:
805 3206.

806 Liu, J., Zheng, Y., Lin, H., Wang, X., Li, M., Liu, Y. et al. (2019) Proliferation of hydrocarbon-
807 degrading microbes at the bottom of the Mariana Trench. *Microbiome* **7**: 47.

808 M. Corn, S.B., F. Partensky, N. Simon and U. Christaki (1996) *Origin and importance of*
809 *picoplanktonic DMSP*: Springer, Boston, MA.

810 Otte, M.L., Wilson, G., Morris, J.T., and Moran, B.M. (2004) Dimethylsulphoniopropionate
811 (DMSP) and related compounds in higher plants. *J Exp Bot* **55**: 1919-1925.

812 Peng, M., Xie, Q., Hu, H., Hong, K., Todd, J.D., Johnston, A.W., and Li, Y. (2012) Phylogenetic
813 diversity of the dddP gene for dimethylsulfoniopropionate-dependent dimethyl sulfide
814 synthesis in mangrove soils. *Can J Microbiol* **58**: 523-530.

815 Raina, J.B., Dinsdale, E.A., Willis, B.L., and Bourne, D.G. (2010) Do the organic sulfur
816 compounds DMSP and DMS drive coral microbial associations? *Trends Microbiol* **18**: 101-
817 108.

818 Raina, J.B., Tapiolas, D.M., Foret, S., Lutz, A., Abrego, D., Ceh, J. et al. (2013) DMSP
819 biosynthesis by an animal and its role in coral thermal stress response. *Nature* **502**: 677-680.

820 Rhodes, D., Gage, D.A., Cooper, A., and Hanson, A.D. (1997) S-methylmethionine conversion
821 to dimethylsulfoniopropionate: Evidence for an unusual transamination reaction. *Plant Physiol*
822 **115**: 1541-1548.

823 Simó, R., and Pedrós-Alió, C. (1999) Role of vertical mixing in controlling the oceanic
824 production of dimethyl sulphide. *Nature* **402**: 396-399.

825 Song, D., Zhang, Y., Liu, J., Zhong, H., Zheng, Y., Zhou, S. et al. (2020) Metagenomic insights
826 into the cycling of dimethylsulfoniopropionate and related molecules in the eastern China
827 marginal seas. *Front Microbiol* **11**: 157.

828 Stefels, J. (2000) Physiological aspects of the production and conversion of DMSP in marine
829 algae and higher plants. *J Sea Res* **43**: 183-197.

830 Sun, H., Zhang, Y., Tan, S., Zheng, Y., Zhou, S., Ma, Q.Y. et al. (2020) DMSP-producing
831 bacteria are more abundant in the surface microlayer than subsurface seawater of the East China
832 Sea. *Microb Ecol* **80**: 350-365.

833 Sun, J., Todd, J.D., Thrash, J.C., Qian, Y., Qian, M.C., Temperton, B. et al. (2016) The abundant
834 marine bacterium Pelagibacter simultaneously catabolizes dimethylsulfoniopropionate to the
835 gases dimethyl sulfide and methanethiol. *Nat Microbiol* **1**: 16065.

836 Sun, L., Curson, A.R.J., Todd, J.D., and Johnston, A.W.B. (2011) Diversity of DMSP transport
837 in marine bacteria, revealed by genetic analyses. *Biogeochemistry* **110**: 121-130.

838 Tan, T.-T., Wu, X., Liu, C.-Y., and Yang, G.-P. (2017) Distributions of dimethylsulfide and its
839 related compounds in the Yangtze (Changjiang) River Estuary and its adjacent waters in early
840 summer. *Cont Shelf Res* **146**: 89-101.

841 Thume, K., Gebser, B., Chen, L., Meyer, N., Kieber, D.J., and Pohnert, G. (2018) The
842 metabolite dimethylsulfoxonium propionate extends the marine organosulfur cycle. *Nature* **563**:
843 412-415.

844 Todd, J.D., Curson, A.R., Dupont, C.L., Nicholson, P., and Johnston, A.W. (2009) The dddP
845 gene, encoding a novel enzyme that converts dimethylsulfoniopropionate into dimethyl sulfide,
846 is widespread in ocean metagenomes and marine bacteria and also occurs in some Ascomycete
847 fungi. *Environ Microbiol* **11**: 1376-1385.

848 Todd, J.D., Curson, A.R., Kirkwood, M., Sullivan, M.J., Green, R.T., and Johnston, A.W. (2011)
849 DddQ, a novel, cupin-containing, dimethylsulfoniopropionate lyase in marine roseobacters and
850 in uncultured marine bacteria. *Environ Microbiol* **13**: 427-438.

851 Tripp, H.J., Kitner, J.B., Schwalbach, M.S., Dacey, J.W., Wilhelm, L.J., and Giovannoni, S.J.
852 (2008) SAR11 marine bacteria require exogenous reduced sulphur for growth. *Nature* **452**:
853 741-744.

854 Uchida, A., Ooguri, T., Ishida, T., Kitaguchi, H., and Ishida, Y. (1996) Biosynthesis of
855 dimethylsulfoniopropionate in Crypthecodinium Cohnii (Dinophyceae). *Planta* **199**: 433-438.

856 Van Alstyne, K.L., and Puglisi, M.P. (2007) DMSP in marine macroalgae and
857 macroinvertebrates: Distribution, function, and ecological impacts. *Aquat Sci* **69**: 394-402.

858 Varaljay, V.A., Howard, E.C., Sun, S., and Moran, M.A. (2010) Deep sequencing of a
859 dimethylsulfoniopropionate-degrading gene (dmdA) by using PCR primer pairs designed on
860 the basis of marine metagenomic data. *Appl Environ Microbiol* **76**: 609-617.

861 Varaljay, V.A., Gifford, S.M., Wilson, S.T., Sharma, S., Karl, D.M., and Moran, M.A. (2012)
862 Bacterial dimethylsulfoniopropionate degradation genes in the oligotrophic north pacific
863 subtropical gyre. *Appl Environ Microbiol* **78**: 2775-2782.

864 Vorobev, A., Dupouy, M., Carradec, Q., Delmont, T.O., Annamale, A., Wincker, P., and Pelletier,
865 E. (2020) Transcriptome reconstruction and functional analysis of eukaryotic marine plankton
866 communities via high-throughput metagenomics and metatranscriptomics. *Genome Res* **30**:
867 647-659.

868 Walters, W., Hyde, E.R., Berg-Lyons, D., Ackermann, G., Humphrey, G., Parada, A. et al. (2016)
869 Improved bacterial 16S rRNA gene (V4 and V4-5) and fungal internal transcribed spacer
870 marker gene primers for microbial community surveys. *mSystems* **1**: e00009-00015.

871 Wilkening, J.V., Turchyn, A.V., Redeker, K.R., Mills, J.V., Antler, G., Carrión, O., and Todd,
872 J.D. (2019) The production and fate of volatile organosulfur compounds in sulfidic and
873 ferruginous sediment. *J Geophys Res-Biogeo* **124**: 3390-3402.

874 Williams, B.T., Cowles, K., Bermejo Martinez, A., Curson, A.R.J., Zheng, Y., Liu, J. et al.

(2019) Bacteria are important dimethylsulfoniopropionate producers in coastal sediments. *Nat Microbiol* **4**: 1815-1825.

Yang, G.-P., Zhang, H.-H., Zhou, L.-M., and Yang, J. (2011) Temporal and spatial variations of dimethylsulfide (DMS) and dimethylsulfoniopropionate (DMSP) in the East China Sea and the Yellow Sea. *Cont Shelf Res* **31**: 1325-1335.

Yin, Q., Fu, B., Li, B., Shi, X., Inagaki, F., and Zhang, X.H. (2013) Spatial variations in microbial community composition in surface seawater from the ultra-oligotrophic center to rim of the South Pacific Gyre. *PLoS One* **8**: e55148.

Zeng, Y.X., Qiao, Z.Y., Yu, Y., Li, H.R., and Luo, W. (2016) Diversity of bacterial dimethylsulfoniopropionate degradation genes in surface seawater of Arctic Kongsfjorden. *Sci Rep* **6**: 33031.

Zhai, W.-D., Yan, X.-L., and Qi, D. (2017) Biogeochemical generation of dissolved inorganic carbon and nitrogen in the North Branch of inner Changjiang Estuary in a dry season. *Estuar Coast Shelf Sci* **197**: 136-149.

Zhang, S.H., Yang, G.P., Zhang, H.H., and Yang, J. (2014a) Spatial variation of biogenic sulfur in the south Yellow Sea and the East China Sea during summer and its contribution to atmospheric sulfate aerosol. *Sci Total Environ* **488-489**: 157-167.

Zhang, X.H., Liu, J., Liu, J., Yang, G., Xue, C.X., Curson, A.R.J., and Todd, J.D. (2019) Biogenic production of DMSP and its degradation to DMS-their roles in the global sulfur cycle. *Sci China Life Sci* **62**: 1296-1319.

Zhang, Y., Zhao, Z., Dai, M., Jiao, N., and Herndl, G.J. (2014b) Drivers shaping the diversity and biogeography of total and active bacterial communities in the South China Sea. *Mol Ecol* **23**: 2260-2274.

Zheng, Y., Jiang, X., Hou, L., Liu, M., Lin, X., Gao, J. et al. (2016) Shifts in the community structure and activity of anaerobic ammonium oxidation bacteria along an estuarine salinity gradient. *J Geophys Res-Biogeo* **121**: 1632-1645.

Zheng, Y., Wang, J., Zhou, S., Zhang, Y., Liu, J., Xue, C.X. et al. (2020) Bacteria are important dimethylsulfoniopropionate producers in marine aphotic and high-pressure environments. *Nat Commun* **11**: 4658.

Zhou, J., Wu, Y., Kang, Q., and Zhang, J. (2007) Spatial variations of carbon, nitrogen, phosphorous and sulfur in the salt marsh sediments of the Yangtze Estuary in China. *Estuar Coast Shelf Sci* **71**: 47-59.

Table 1 The averaged genes abundance of FL and PA bacteria in freshwater, transition and seawater samples of winter and summer.

Genes		16S rRNA			*dsyB*			*mmtN*			*dddP*			*dmdA*		
		Freshwater	Transition	Seawater	Freshwater	Transition	Seawater	Freshwater	Transition	Seawater	Freshwater	Transition	Seawater	Freshwater	Transition	Seawater
Winter	FL	4.34×10^{4}	9.90×10^{4}	2.83×10^{4}	1.34×10^{1}	2.16×10^{2}	2.34×10^{2}	5.76×10^{-1}	3.07×10^{1}	1.42×10^{1}	2.94×10^{2}	7.22×10^{2}	2.10×10^{3}	4.08×10^{2}	1.68×10^{3}	1.83×10^{4}
	PA	4.01×10^{4}	6.16×10^{4}	1.30×10^{5}	6.07×10^{0}	2.26×10^{2}	6.22×10^{1}	1.99×10^{0}	2.99×10^{0}	5.17×10^{0}	1.97×10^{2}	5.48×10^{2}	4.06×10^{2}	2.72×10^{2}	8.98×10^{2}	2.30×10^{3}
Summer	FL	3.63×10^{5}	7.84×10^{4}	5.92×10^{4}	6.96×10^{1}	4.11×10^{2}	8.60×10^{2}	4.36×10^{0}	2.85×10^{0}	2.45×10^{0}	6.67×10^{1}	1.44×10^{4}	1.63×10^{4}	7.49×10^{1}	2.52×10^{4}	1.55×10^{4}
	PA	1.68×10^{5}	1.91×10^{5}	1.20×10^{5}	1.51×10^{1}	8.74×10^{1}	2.93×10^{2}	8.00×10^{-2}	2.80×10^{0}	1.05×10^{0}	1.20×10^{2}	3.69×10^{3}	5.74×10^{2}	2.48×10^{2}	4.78×10^{3}	3.16×10^{3}

*FL, free-living. PA, particle-associated.

Table 2 The gene transcripts abundance of FL and PA bacteria in freshwater, transition and seawater samples of winter and summer.

Transcripts		16S rRNA			*dsyB*			*mmtN*			*dddP*			*dmdA*		
		Freshwater	Transition	Seawater	Freshwater	Transition	Seawater	Freshwater	Transition	Seawater	Freshwater	Transition	Seawater	Freshwater	Transition	Seawater
Winter	FL	1.65×10^{7}	1.36×10^{7}	7.36×10^{7}	0	6.38×10^{1}	4.50×10^{1}	0	3.67×10^{0}	0	7.19×10^{0}	1.58×10^{2}	9.43×10^{1}	7.84×10^{0}	1.79×10^{2}	1.86×10^{2}
	PA	8.38×10^{6}	8.07×10^{6}	7.69×10^{6}	0	2.41×10^{1}	1.92×10^{1}	0	6.55×10^{-1}	8.62×10^{-2}	8.31×10^{0}	4.62×10^{1}	6.97×10^{1}	1.54×10^{0}	1.59×10^{2}	9.91×10^{1}
Summer	FL	7.18×10^{8}	5.31×10^{8}	3.11×10^{8}	0	1.37×10^{1}	1.03×10^{1}	0	3.72×10^{-1}	1.34×10^{0}	7.71×10^{0}	1.52×10^{2}	1.02×10^{2}	4.78×10^{0}	7.75×10^{1}	5.49×10^{2}
	PA	1.95×10^{8}	3.09×10^{8}	2.16×10^{7}	0	6.57×10^{0}	1.45×10^{1}	0	2.82×10^{-1}	0	8.80×10^{0}	1.10×10^{2}	9.06×10^{1}	3.21×10^{0}	2.99×10^{2}	2.39×10^{2}

*FL, free-living. PA, particle-associated.

912 **Table 3** Primers and amplification conditions for qPCR detection and high-through sequencing of bacteria.

Target gene	Primers	Sequences (5'-3')	Amplicon length (bp)	Annealing temp (°C)	Usage	References
16S rRNA	338F 518R	ACTCCTACGGGAGGCAGCAG ATTACCGCGGCTGCTGG	180	53	qPCR	(Yin et al., 2013)
dsyB	dsyBF dsyBR	CATGGGSTCSAAGGCSCTKTT GCAGRTARTCGCCGAAATCGTA	246	61		(Williams et al., 2019) (Williams et al., 2019)
mmtN	mmtNF mmtNR	CCGAGGTGGTCATGAAYTTYGG GGATCACGCACACYTCRTGRTA	301	54		(Williams et al., 2019) (Williams et al., 2019)
dddP	874F 971R	AAYGAAATWGTTGCCTTTGA GCATDGCRTAAATCATATC	97	41		(Levine et al., 2012)
dmdA(C/2)	291F 482R	AGATGAAAATGCTGGAATGATAAATG AAATCTTCAGACTTTGGACCTTG	191	50		(Levine et al., 2012) (Varaljay et al., 2010)
dmdA(D/1)	268F 356R	AGATGTTATTATTGTCCAATAATTGATG ATCCACCATCTATCTTCAGCTA	89	49		(Levine et al., 2012) (Varaljay et al., 2010)
16S rRNA	515modF 806modR	GTGYCAGCMGCCGCGGTAA GGACTACNVGGGTWTCTAAT	291	50	Amplicon sequencing	(Walters et al., 2016)

913

Tables and Figure Legends

Fig. 1 Sampling map in both winter and summer cruises. A, sampling sites. B and C, surface and bottom samples in winter and summer, respectively. Yellow, freshwater samples. Green, transition region water samples. Cyan, seawater samples. Orange in A, variable area that samples were different in summer and winter.

Fig. 2 DMSP concentrations of Changjiang Estuary winter and summer samples. A, B and C, the $DMSP_t$, $DMSP_p$ and $DMSP_d$ of Changjiang Estuary winter samples. D, E and F, the $DMSP_t$, $DMSP_p$ and $DMSP_d$ of Changjiang Estuary summer samples. $DMSP_t$, total DMSP. $DMSP_p$, particulate DMSP, including $DMSP_{p1}$ and $DMSP_{p2}$. $DMSP_{p1}$ was these captured on 3 μm membrane. $DMSP_{p2}$ was these DMSP passed through 3 μm but was captured on the 0.22 μm filter. $DMSP_d$, dissolved DMSP. F, freshwater samples; T, transition water samples; S, seawater samples. The former "W" or "S" of the sample name represents winter or summer samples, while the latter "S" or "B" means surface or bottom water samples.

Fig. 3 DMSP producing and catabolic gene abundance in metagenomes from Changjiang Estuary winter and summer samples.

Fig. 4 The abundance of DMSP producing and catabolic genes and DMSP concentration in Changjiang Estuary winter and summer samples. A and B, *dsyB* gene abundance in winter and summer, respectively. C and D, *mmtN* gene abundance in

winter and summer, respectively. FL, free-living. PA, particle-associated. $DMSP_{p1}$, DMSP was these captured on 3 μm membrane. $DMSP_{p2}$, DMSP passed through 3 μm but was captured on the 0.22 μm filter. F, freshwater samples; T, transition water samples; S, seawater samples.

Fig. 5 The abundance of DMSP producing and catabolic gene transcripts and DMSP/DMS concentrations in Changjiang Estuary summer and winter samples. A, the abundance of *dsyB* transcripts. B, the abundance of *mmtN* transcripts. C, the abundance of *dddP* transcripts. D, the abundance of *dmdA* (C/2 and D/1 subclade) transcripts. FL, free-living. PA, particle-associated. $DMSP_{p1}$, DMSP was these captured on 3 μm membrane. $DMSP_{p2}$, DMSP passed through 3 μm but was captured on the 0.22 μm filter. $DMSP_{d}$, dissolved DMSP. F, freshwater samples; T, transition water samples; S, seawater samples.

Fig. 6 Neighbor-joining tree of representative *dsyB* OTU sequences in Changjiang Estuary winter and summer samples. 192 sequences were used to construct the nucleotide tree. The topologies of phylogenetic tree were evaluated based on the bootstrap resampling method with 1000 replicates. Bootstrap coefficients below 70% were not shown. OTUs of *dsyB* in winter samples were marked with triangle while summer samples were marked with circle. OTUs of *dsyB* in freshwater samples were dyed with orange, transition samples with green and seawater samples with cyan. The abundance of OTUs were indicated by triangle and circle size. Strains experimentally confirmed to produce DMSP are marked with a red square.

Fig. 7 The abundance of DMSP catabolic genes and DMS/DMSP concentrations in Changjiang Estuary winter and summer samples. A and B, the abundance of *dddP* genes in winter and summer samples, respectively. C and D, the abundance of *dmdA* (C/2 and D/1 subclade) genes in winter and summer, respectively. FL, free-living. PA, particle-associated. $DMSP_d$, dissolved DMSP. F, freshwater samples; T, transition water samples; S, seawater samples.

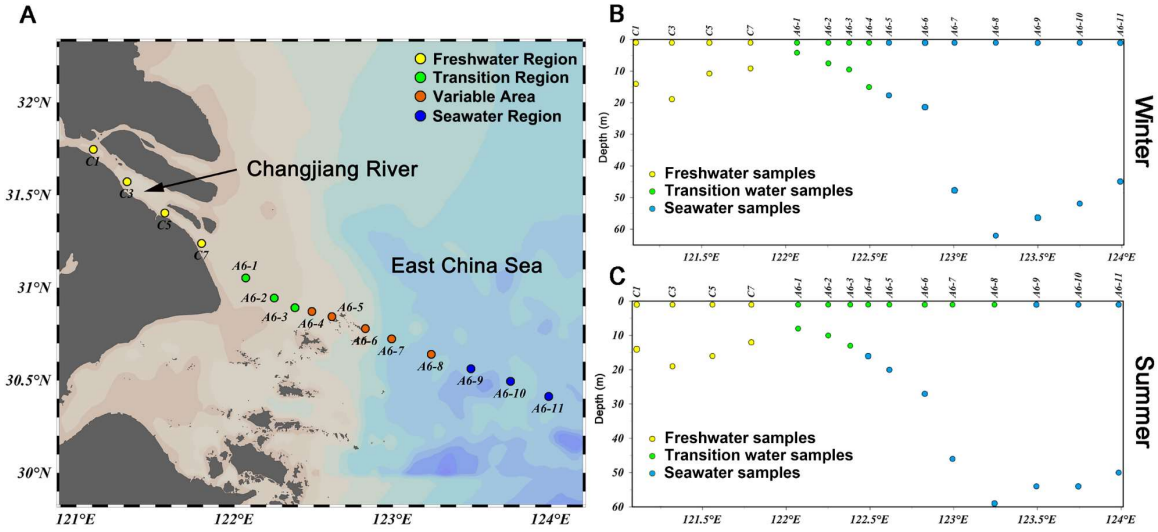

Fig. 1 Sampling map in both winter and summer cruises. A, sampling sites. B and C, surface and bottom samples in winter and summer, respectively. Yellow, fresh water samples. Green, transition region water samples. Cyan, seawater samples. Orange in A, variable area that samples were different in summer and winter.

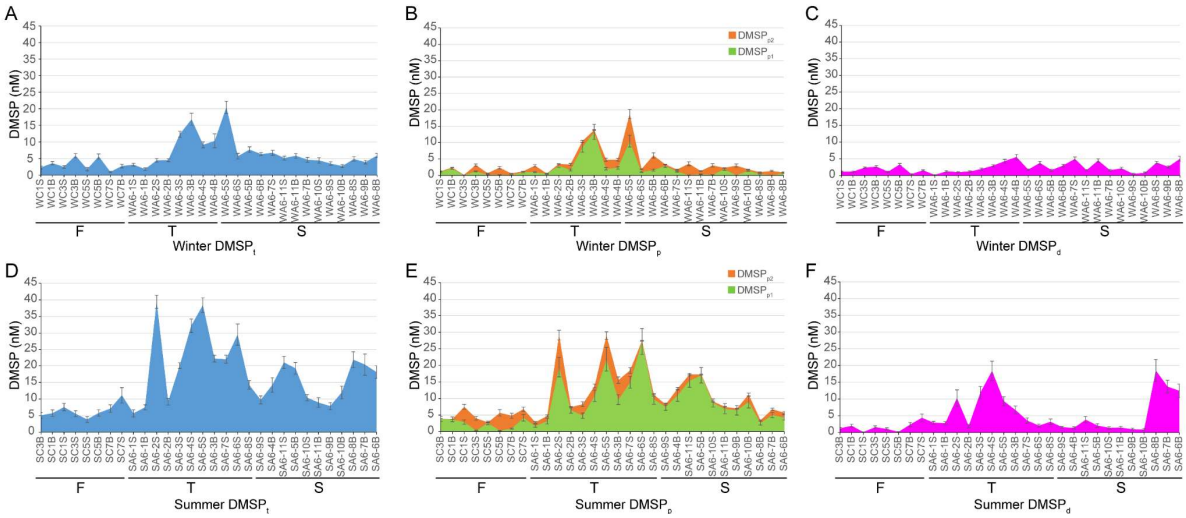

Fig. 2 DMSP concentrations of the Changjiang Estuary in winter and summer. A, B and C, the $DMSP_t$, $DMSP_p$ and $DMSP_d$ in winter of the Changjiang Estuary. D, E and F, the $DMSP_t$, $DMSP_p$ and $DMSP_d$ in summer of the Changjiang Estuary. $DMSP_t$, total DMSP. $DMSP_p$, particulate DMSP, including $DMSP_{p1}$ and $DMSP_{p2}$. $DMSP_{p1}$ was these captured on 3 μm membrane. $DMSP_{p2}$ was these DMSP passed through 3 μm but was captured on the 0.22 μm filter. $DMSP_d$, dissolved DMSP. F, freshwater samples; T, transition water samples; S, seawater samples. The former "W" or "S" of the sample name represents winter or summer samples, while the latter "S" or "B" means surface or bottom water samples.

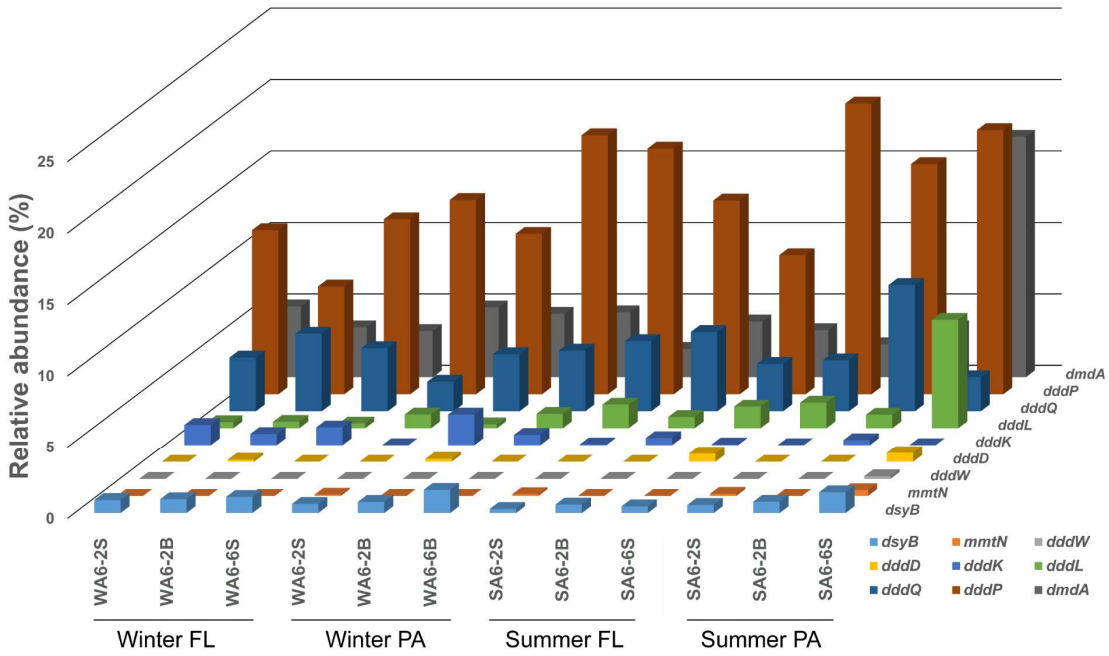

Fig. 3 The DMSP producing and catabolic gene abundance in the metagenomes from winter and summer samples.

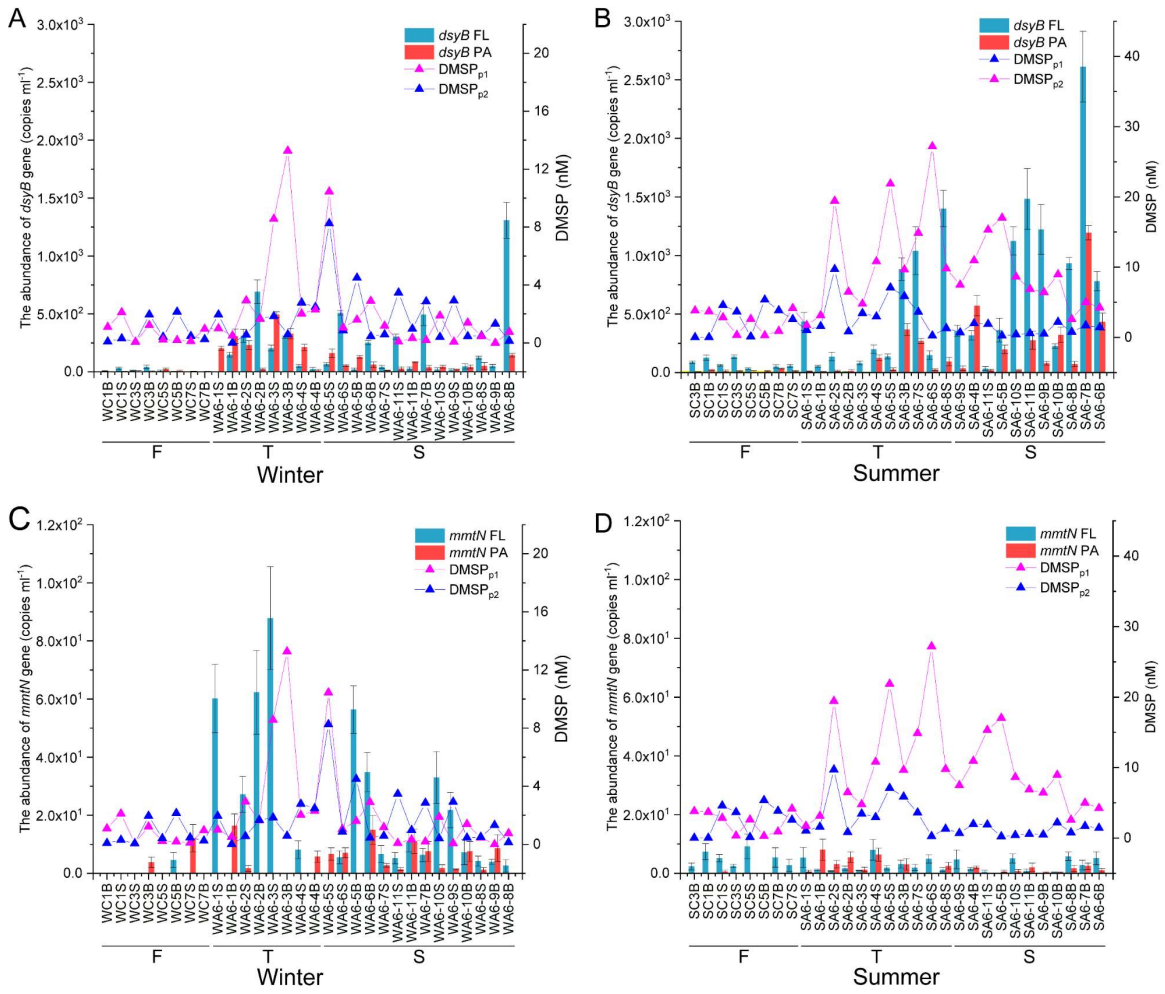

Fig. 4 The abundance of DMSP producing and catabolic genes and DMSP concentration in winter and summer Changjiang Estuary samples. A and B, *dsyB* gene abundance in winter and summer, respectively. C and D, *mmtN* gene abundance in winter and summer, respectively. FL, free-living. PA, particle-associated. $DMSP_{p1}$, DMSP was these captured on 3 μm membrane. $DMSP_{p2}$, DMSP passed through 3 μm but was captured on the 0.22 μm filter. F, freshwater samples; T, transition water samples; S, seawater samples.

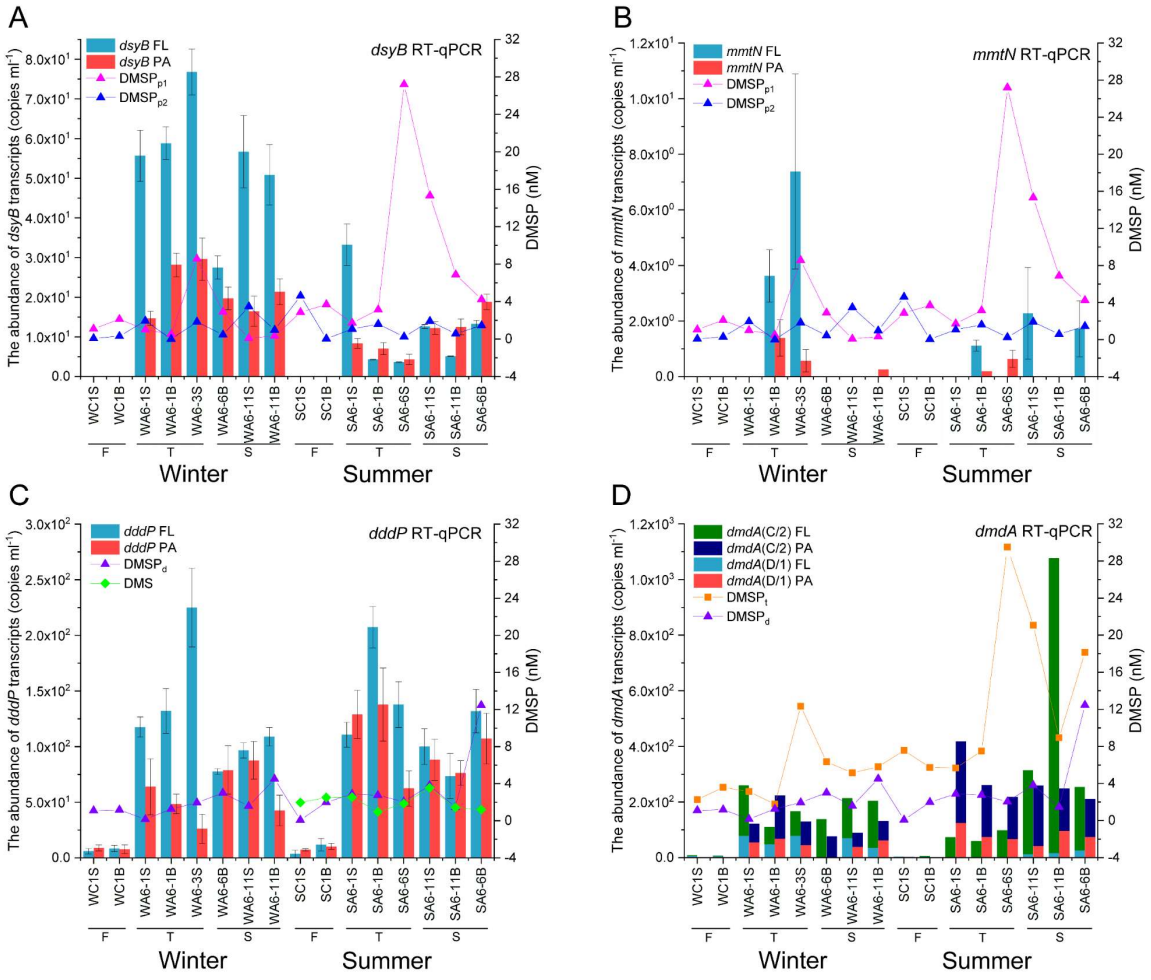

Fig. 5 The abundance of DMSP producing and catabolic gene transcripts and DMSP/DMS concentrations in summer and winter Changjiang Estuary samples. A, the abundance of *dsyB* transcripts. B, the abundance of *mmtN* transcripts. C, the abundance of *dddP* transcripts. D, the abundance of *dmdA* (C/2 and D/1 subclade) transcripts. FL, free-living. PA, particle-associated. $DMSP_{p1}$, DMSP was these captured on 3 μm membrane. $DMSP_{p2}$, DMSP passed through 3 μm but was captured on the 0.22 μm filter. $DMSP_d$, dissolved DMSP. F, freshwater samples; T, transition water samples; S, seawater samples.

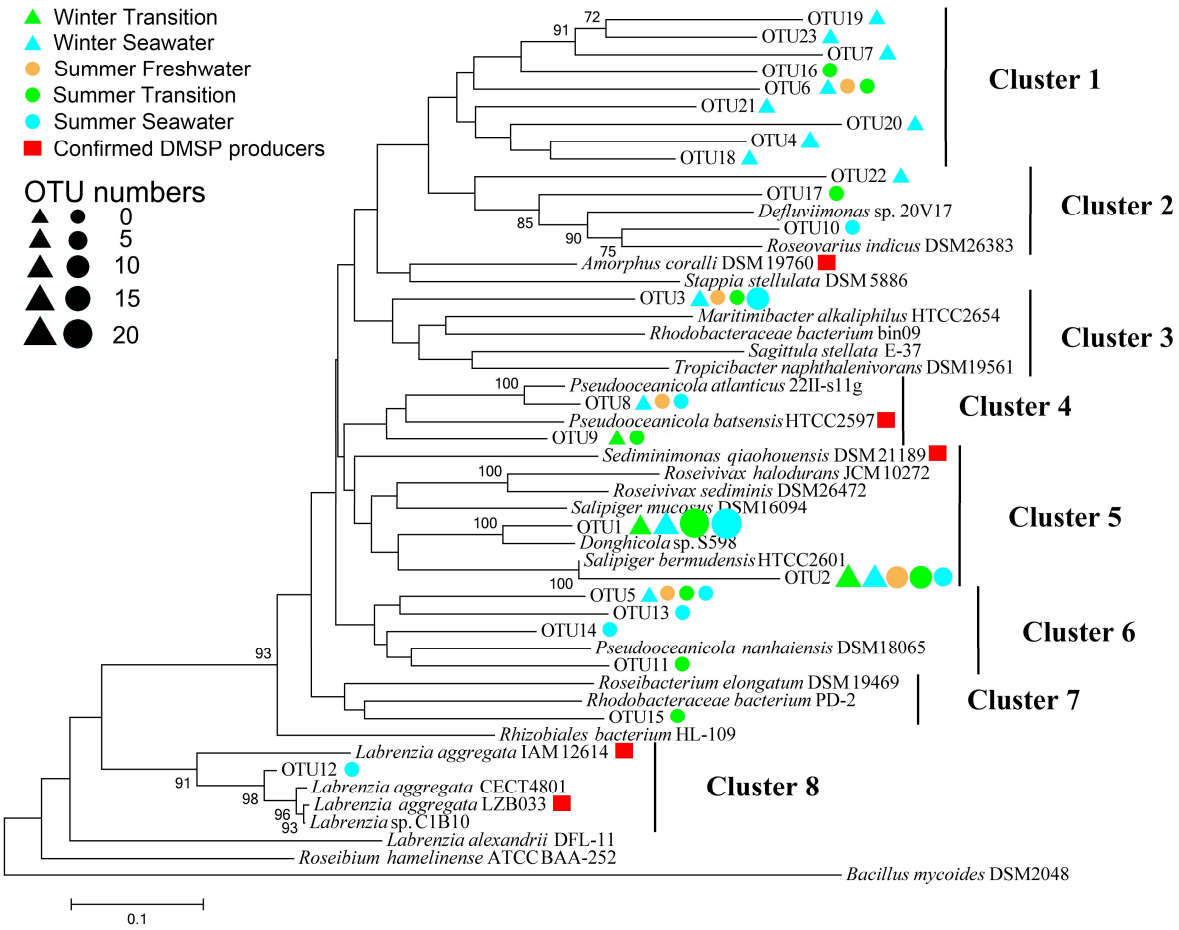

Fig. 6 Neighbor-joining tree of representative *dsyB* OTU sequences in winter and summer Changjiang Estuary samples. 192 sequences were used to construct the nucleotide tree. The topologies of phylogenetic tree were evaluated based on the bootstrap resampling method with 1000 replicates. Bootstrap coefficients below 70% were not shown. OTUs of *dsyB* in winter samples were marked with triangle while summer samples were marked with circle. OTUs of *dsyB* in freshwater samples were dyed with orange, transition samples with green and seawater samples with cyan. The abundance of OTUs were indicated by triangle and circle size. Strains experimentally confirmed to produce DMSP are marked with a red square.

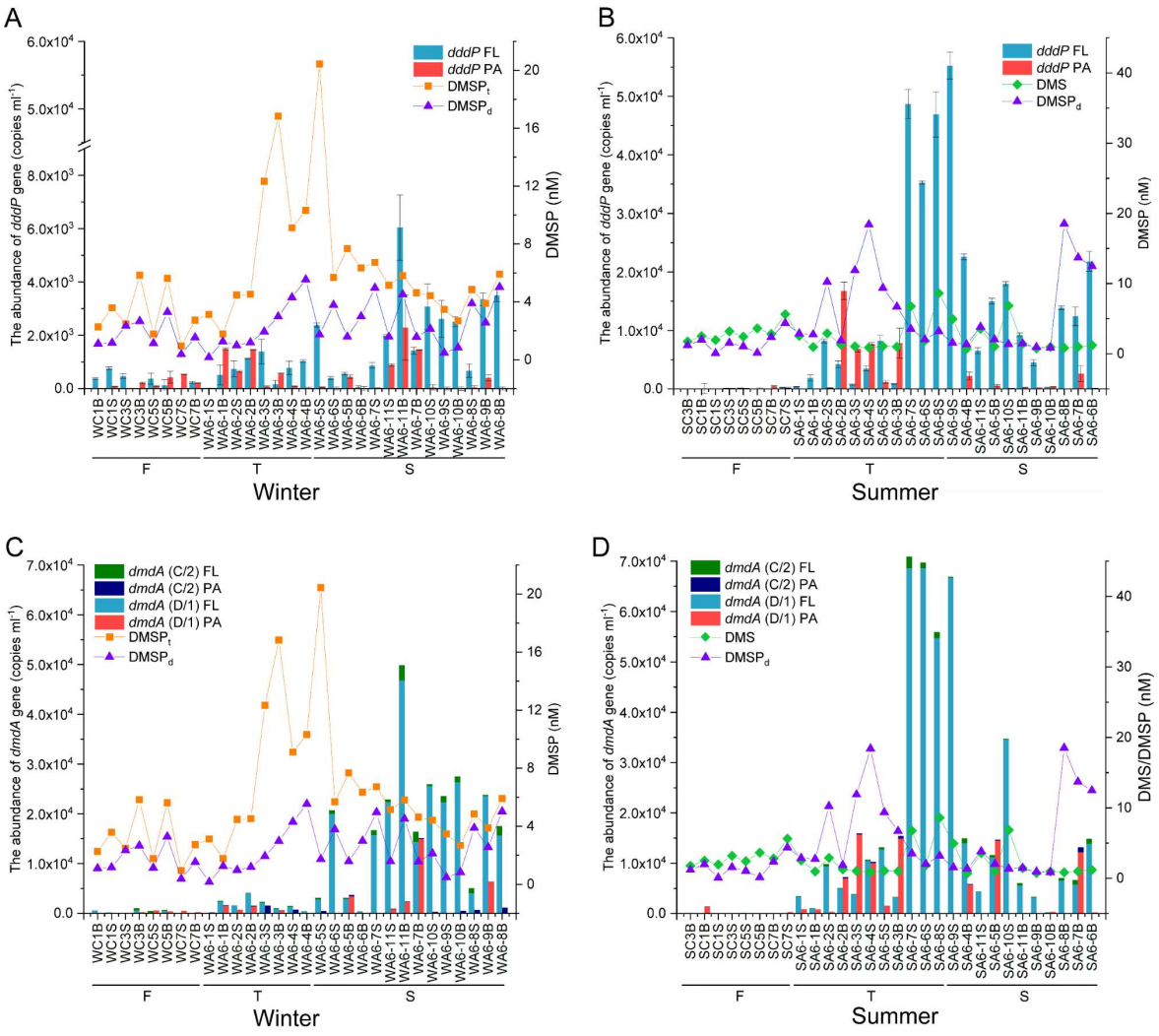

Fig. 7 The abundance of DMSP catabolic genes and DMS/DMSP concentrations in winter and summer Changjiang Estuary samples. A and B, the abundance of *dddP* genes in winter and summer samples, respectively. C and D, the abundance of *dmdA* (C/2 and D/1 subclade) genes in winter and summer, respectively. FL, free-living. PA, particle-associated. $DMSP_d$, dissolved DMSP. F, freshwater samples; T, transition water samples; S, seawater samples.

Spatiotemporal distribution of bacterial DMSP producing and catabolic genes in the Changjiang Estuary

Hao Sun[1,2], Ji Liu[1], Siyin Tan[1], Yanfen Zheng[1], Xiaolei Wang[1], Jinchang Liang[1], Jonathan D. Todd[3*] and Xiao-Hua Zhang[1,2,4*]

[1]College of Marine Life Sciences, and Frontiers Science Center for Deep Ocean Multispheres and Earth System, Ocean University of China, 5 Yushan Road, Qingdao 266003, China

[2]Laboratory for Marine Ecology and Environmental Science, Qingdao National Laboratory for Marine Science and Technology, Qingdao 266071, China

[3]School of Biological Sciences, University of East Anglia, Norwich Research Park, Norwich, NR47TJ, UK

[4]Institute of Evolution & Marine Biodiversity, Ocean University of China, Qingdao 266003, China

***Correspondence:**

Xiao-Hua Zhang, xhzhang@ouc.edu.cn; Dr. Jonathan D. Todd, jonathan.todd@uea.ac.uk

Supplementary Figures

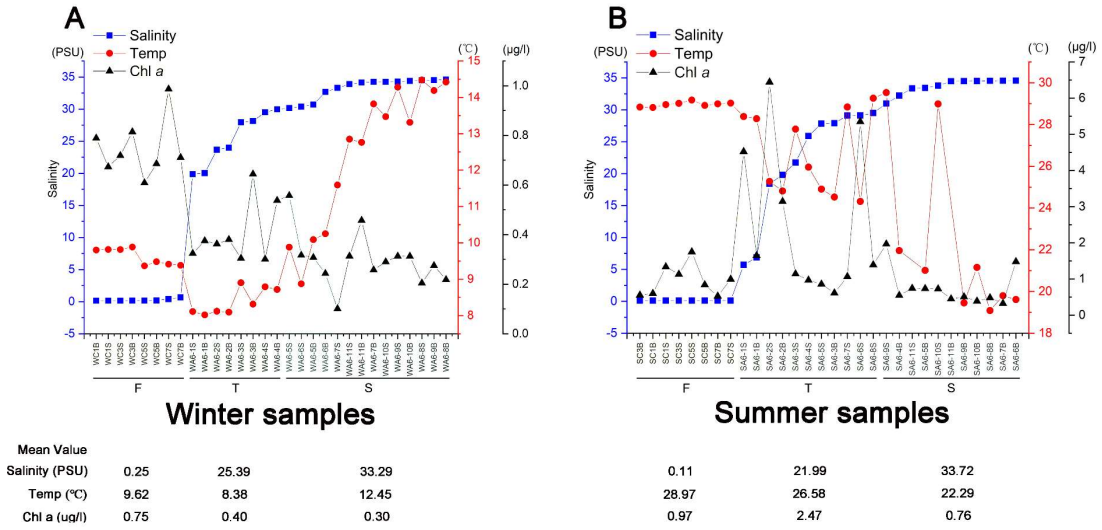

Mean Value						
Salinity (PSU)	0.25	25.39	33.29	0.11	21.99	33.72
Temp (℃)	9.62	8.38	12.45	28.97	26.58	22.29
Chl a (ug/l)	0.75	0.40	0.30	0.97	2.47	0.76

Fig. S1 The salinity, temperature and Chl *a* levels in Changjiang Estuary winter and summer samples. A, winter samples. B, summer samples. F, freshwater samples; T, transition water samples; S, seawater samples.

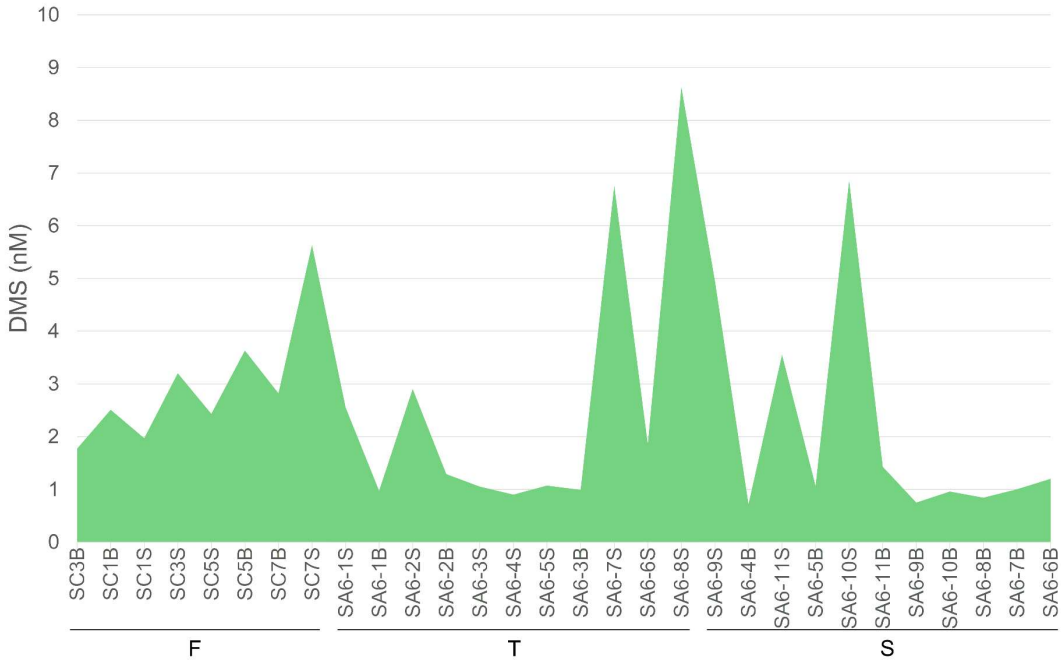

Fig. S2 DMS concentration from Changjiang Estuary summer samples. Yellow, fresh water samples. F, freshwater samples; T, transition water samples; S, seawater samples.

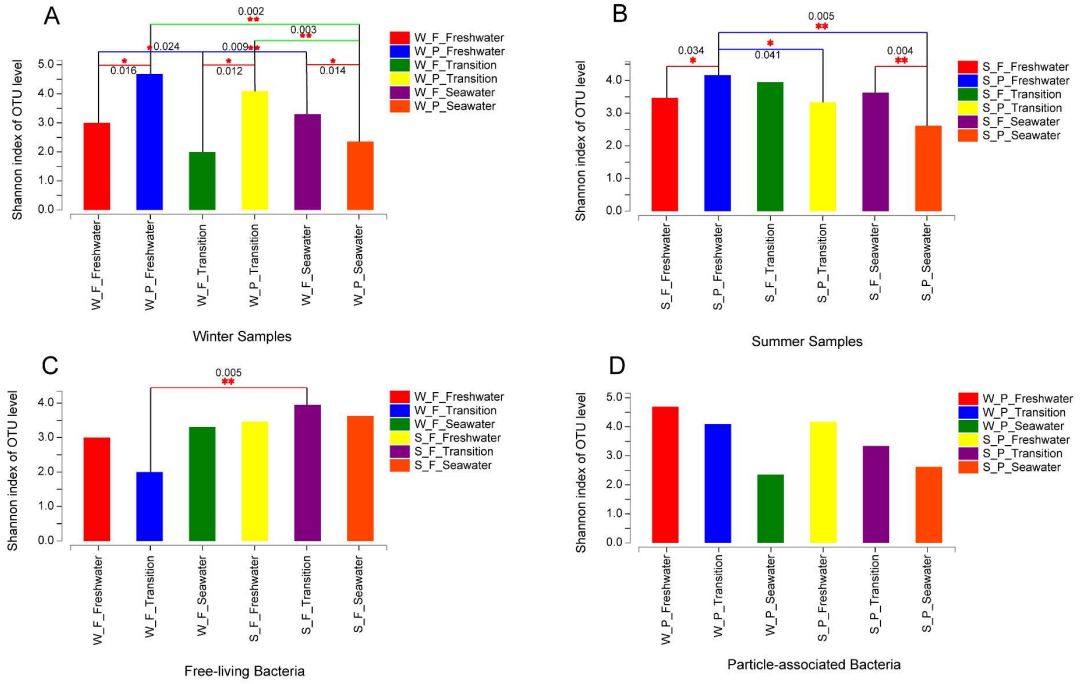

Fig. S3 The difference of Shannon index between seasons, among regions and between free-living and particle-associated bacteria. A, the difference between free-living and particle-associated bacteria and among regions of winter samples. B, the difference between free-living and particle-associated bacteria and among regions of summer samples. C, the difference between winter and summer samples of free-living bacteria in three regions. D, the difference between winter and summer samples of particle-associated bacteria in three regions. W, winter. S, summer. F, free-living. P, particle-associated. $P < 0.05$ was marked with "*". $P < 0.01$ was marked with "**".

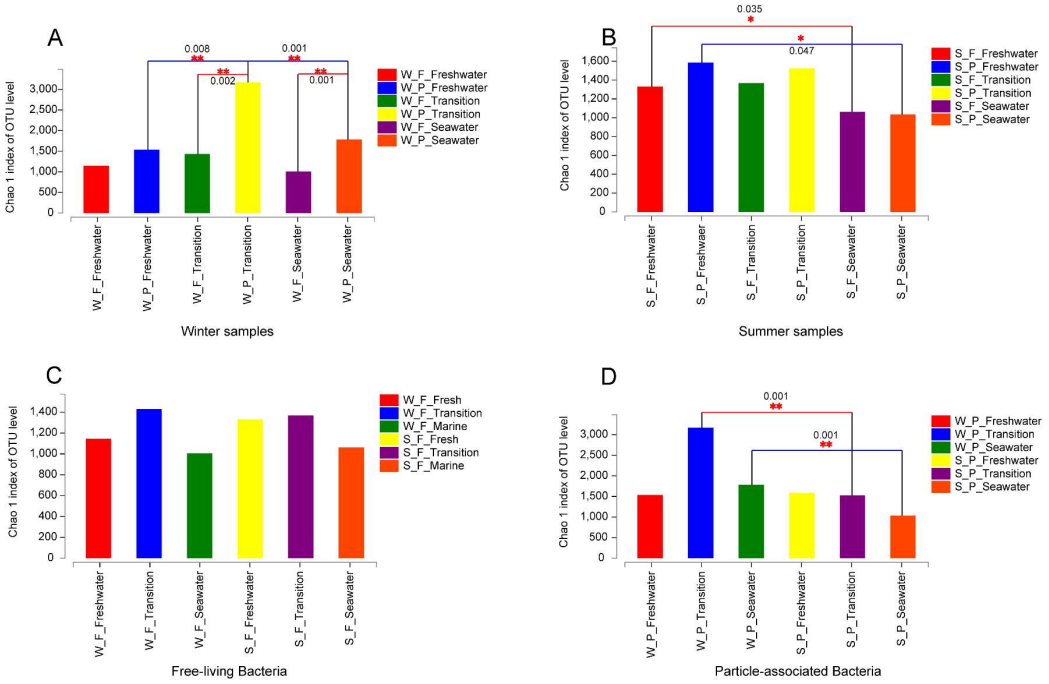

Fig. S4 The difference of Chao 1 index between seasons, among regions and between free-living and particle-associated bacteria. A, the difference between free-living and particle-associated bacteria and among regions of winter samples. B, the difference between free-living and particle-associated bacteria and among regions of summer samples. C, the difference between winter and summer samples of free-living bacteria in three regions. D, the difference between winter and summer samples of particle-associated bacteria in three regions. W, winter. S, summer. F, free-living. P, particle-associated. $P < 0.05$ was marked with "*". $P < 0.01$ was marked with "**".

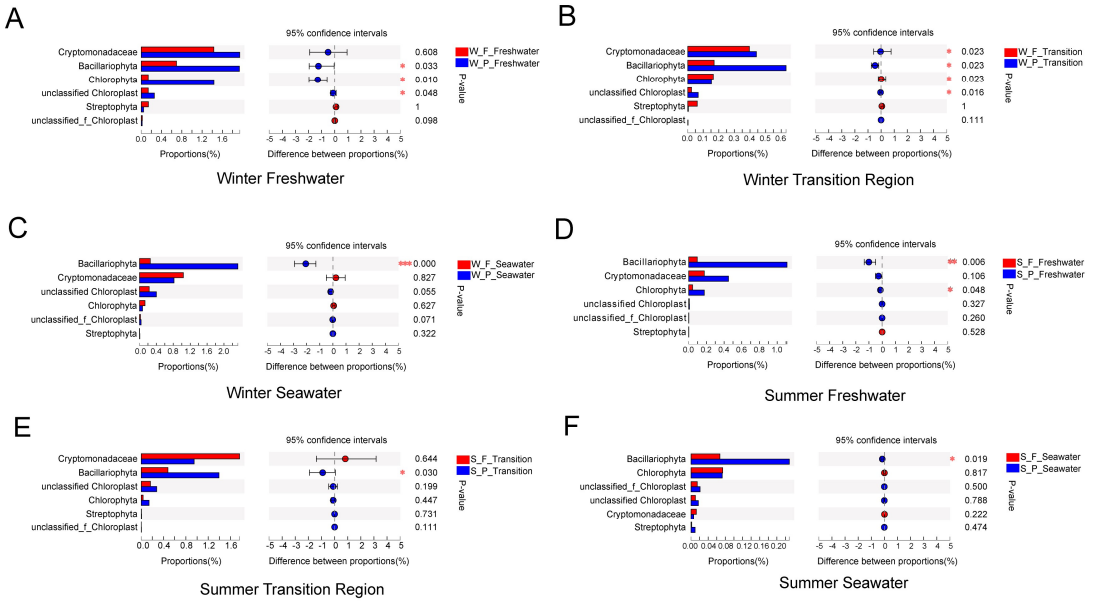

Fig. S5 The proportion of plastids sequences in 16S rRNA data from free-living and particle-associated fractions of winter and summer samples. A, freshwater samples in winter. B, transition region water samples in winter. C, seawater samples in winter. D, freshwater samples in summer. E, transition region water samples in summer. F, seawater samples in summer. W, winter. S, summer. F, free-living. P, particle-associated. $P < 0.05$ was marked with "*". $P < 0.01$ was marked with "**"

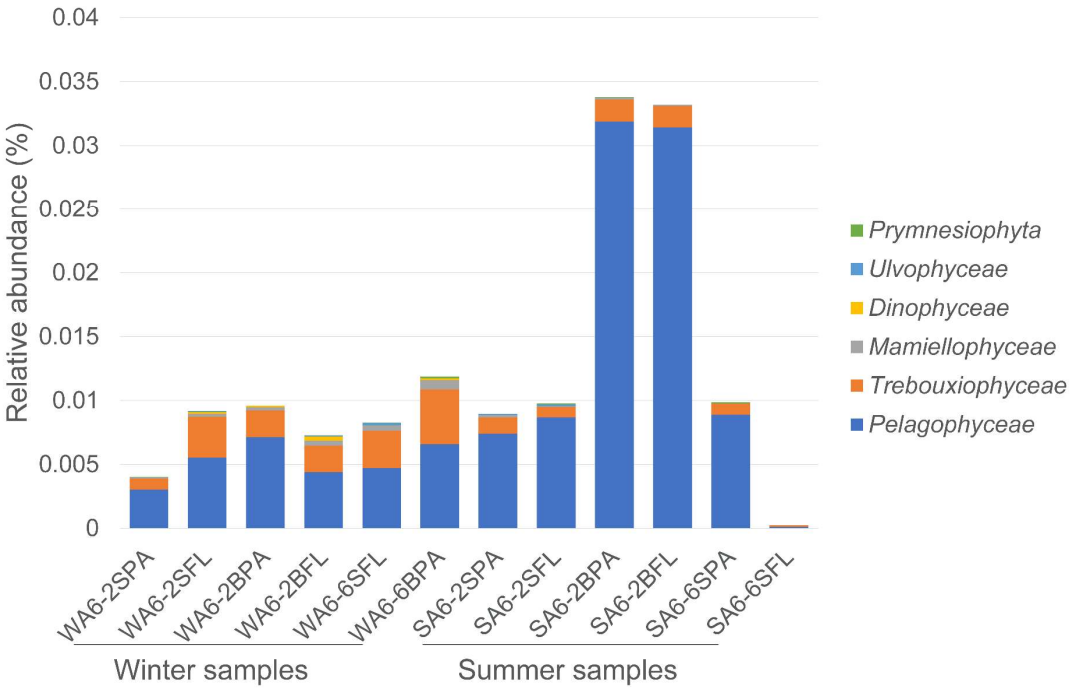

Fig. S6 The relative abundance of eukaryotic algae in metagenome data at the class level. SPA, surface particle-associated samples. SFL, surface free-living samples. BPA, bottom particle-associated samples. BFL, bottom free-living samples.

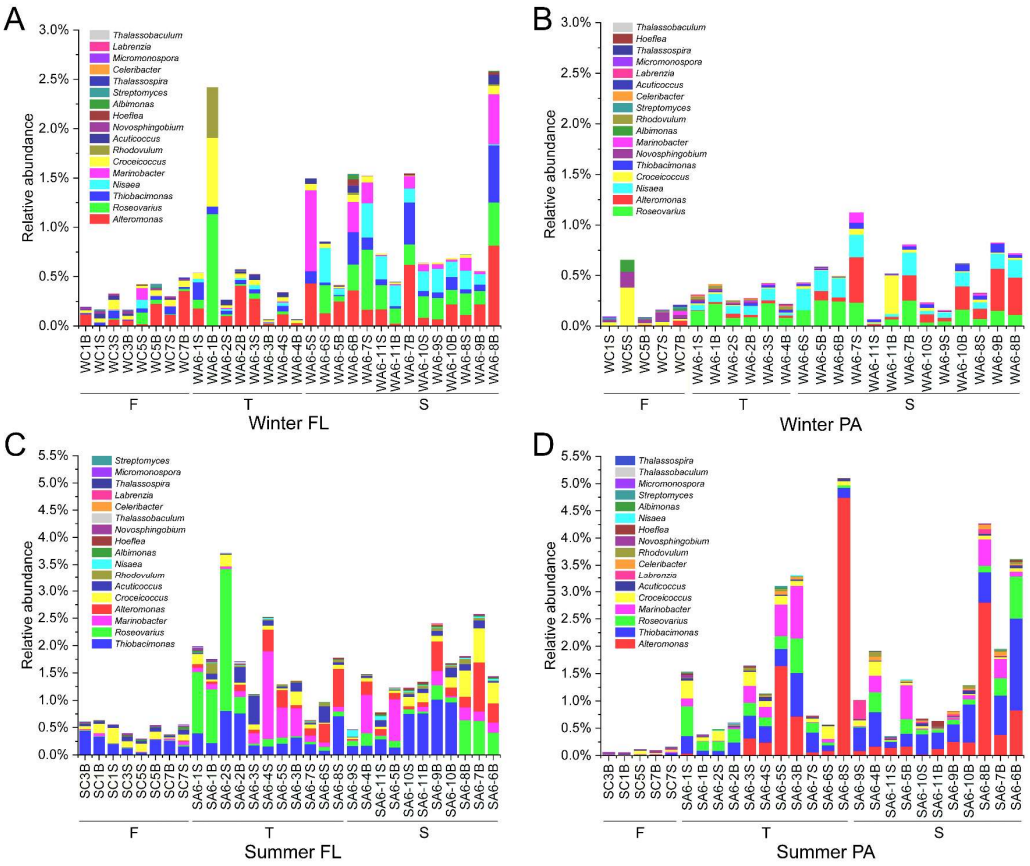

Fig. S7 The relative abundance of DMSP producing genera in winter and summer samples. A, Predicted DMSP producing bacterial genera in the free-living fractions of winter samples. B, Predicted DMSP producing bacterial genera in the particle-associated fractions of winter samples. C, Predicted DMSP producing bacterial genera in free-living fractions in summer samples. D, DMSP producing bacterial genera in particle-associated fractions of summer samples. FL, free-living. PA, particle-associated. The same genera are marked with the same color. F, freshwater samples; T, transition water samples; S, seawater samples.

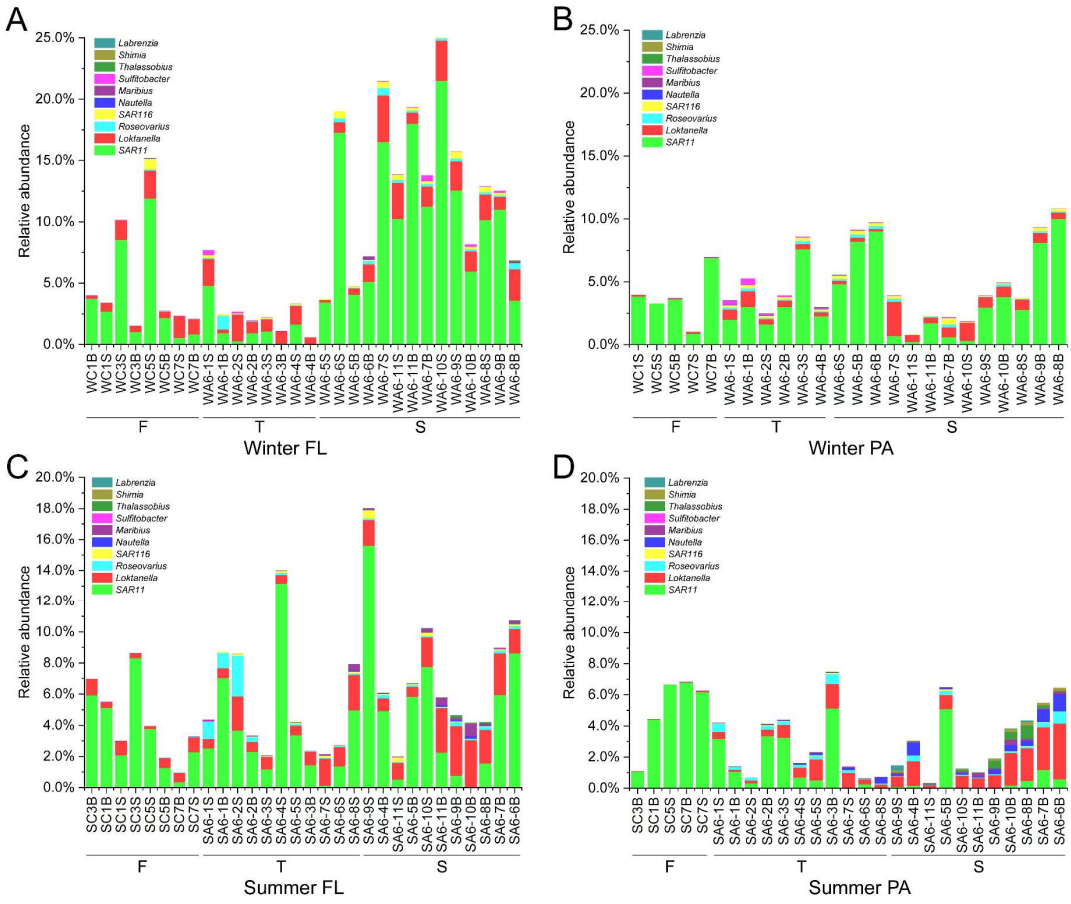

Fig. S8 The relative abundance of DMSP catabolic bacteria in winter and summer samples. A, DMSP catabolic bacteria of free-living fractions in winter samples. B, DMSP catabolic bacteria of particle-associated fractions in winter samples. C, DMSP catabolic bacteria of free-living fractions in summer samples. D, DMSP catabolic bacteria of particle-associated fractions in summer samples. FL, free-living. PA, particle-associated. The same bacteria were marked with the same color. F, freshwater samples; T, transition water samples; S, seawater samples.

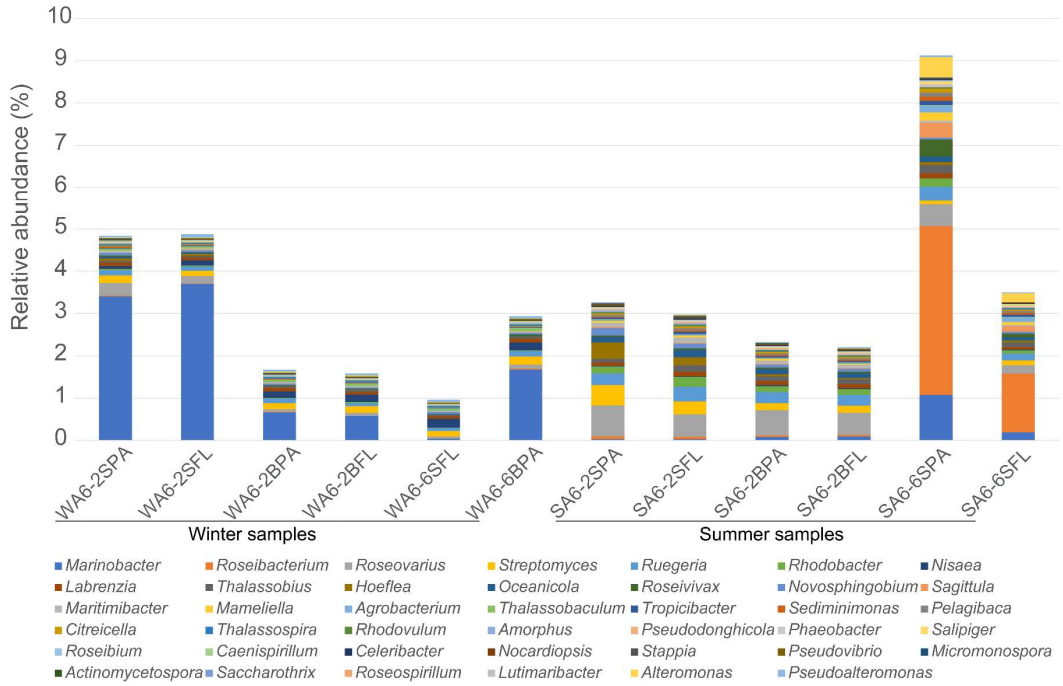

Fig. S9 The relative abundance of DMSP producing genera in metagenome data from the Changjiang Estuary. SPA, surface particle-associated samples. SFL, surface free-living samples. BPA, bottom particle-associated samples. BFL, bottom free-living samples.

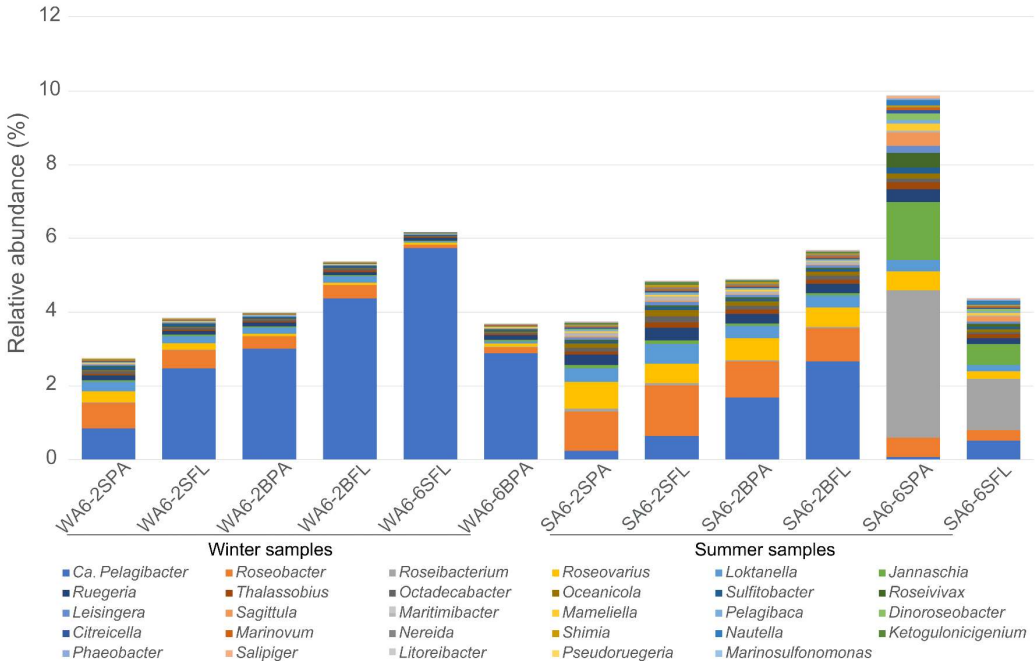

Fig. S10 The relative abundance of DMSP catabolic genera in metagenome data from the Changjiang Estuary. SPA, surface particle-associated samples. SFL, surface free-living samples. BPA, bottom particle-associated samples. BFL, bottom free-living samples.

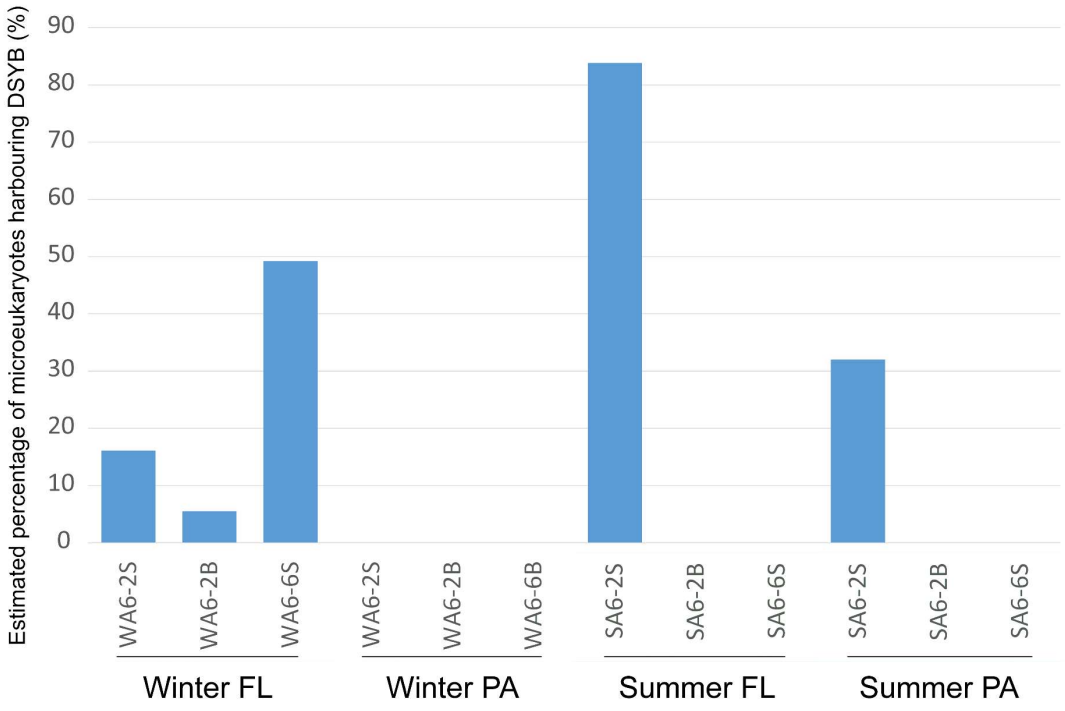

Fig. S11 The relative abundance of *DSYB* in metagenome data from the Changjiang Estuary. *DSYB* abundance was normalised to the number of β-Actin sequences. FL, free-living samples; PA, particle-associated samples.

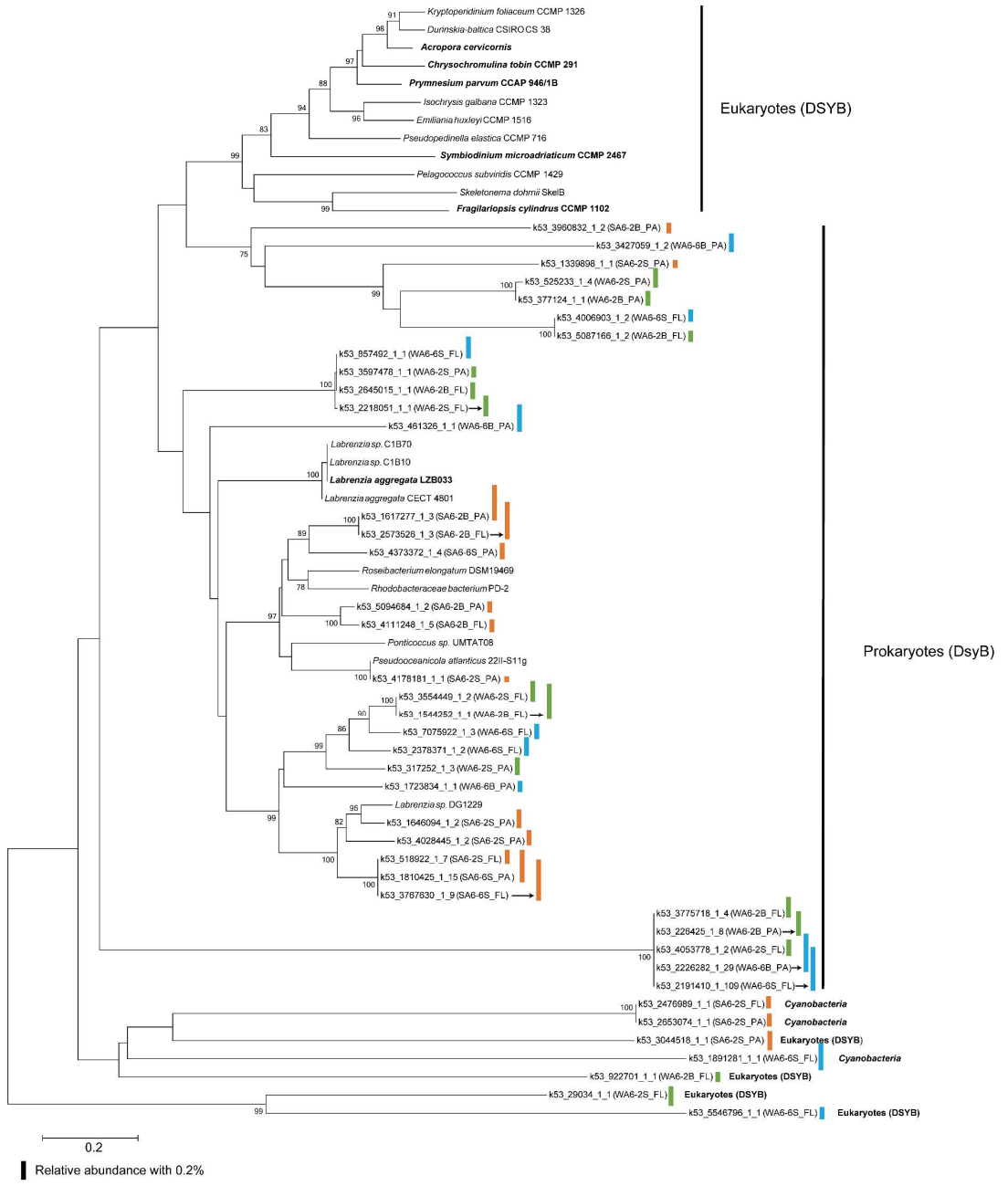

Fig. S12 Neighbor-Joining phylogenetic tree of DsyB/DSYB proteins from metagenome data. 62 protein sequences were used to construct the protein tree. The topologies of phylogenetic tree were evaluated based on the bootstrap resampling method with 1000 replicates. Bootstrap coefficients below 70% were not shown. The sample names were marked after the sequences. PA, particle-associated. FL, free-living. The relative abundance of protein sequences was indicated by bars. Orange bar, transition samples of summer. Green bar, transition samples of winter. The proteins shown to be functional were marked in bold.

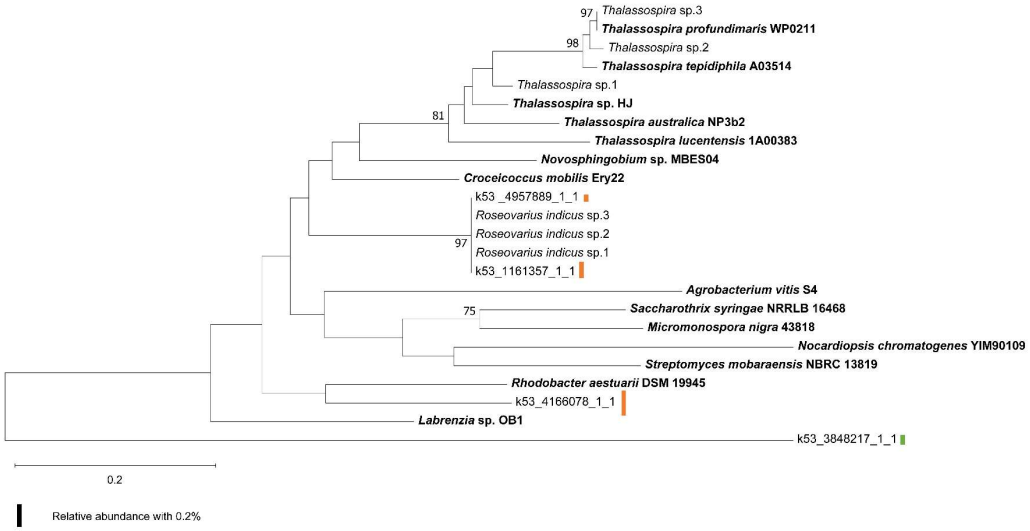

Fig. S13 Neighbor-Joining phylogenetic tree of MmtN proteins from metagenome data. 24 protein sequences were used to construct the protein tree. The topologies of phylogenetic tree were evaluated based on the bootstrap resampling method with 1000 replicates. Bootstrap coefficients below 70% were not shown. The relative abundance of protein sequences was indicated by bars. Orange bar, transition samples of summer. Green bar, transition samples of winter. The proteins shown to be functional were marked in bold.

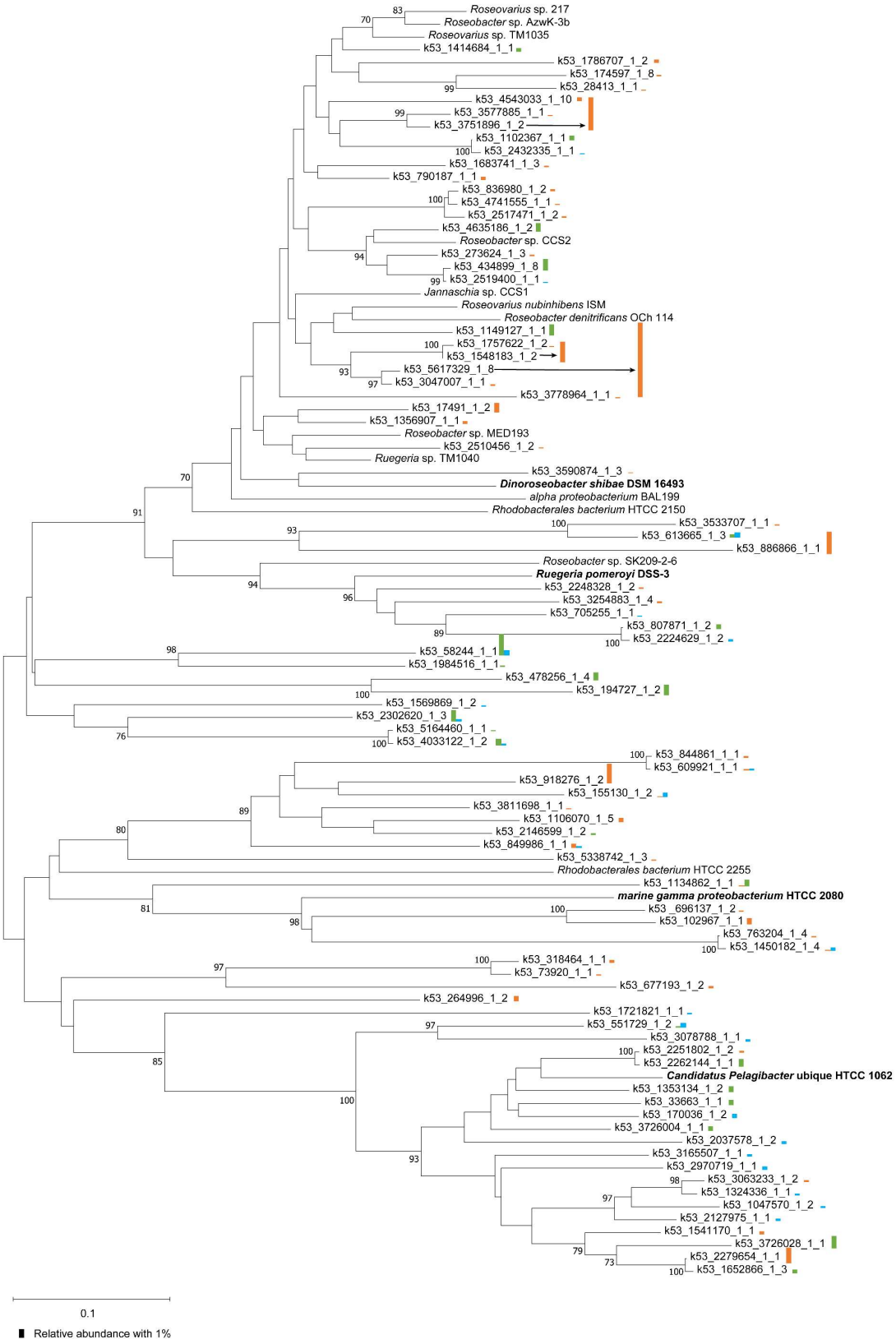

Fig. S14 Neighbor-Joining phylogenetic tree of DmdA proteins from metagenome data. 99 protein sequences were used to construct the protein tree. The topologies of

phylogenetic tree were evaluated based on the bootstrap resampling method with 1000 replicates. Bootstrap coefficients below 70% were not shown. The relative abundance of protein sequences was indicated by bars. Orange bar, transition samples of summer. Green bar, transition samples of winter. The proteins shown to be functional were marked in bold.

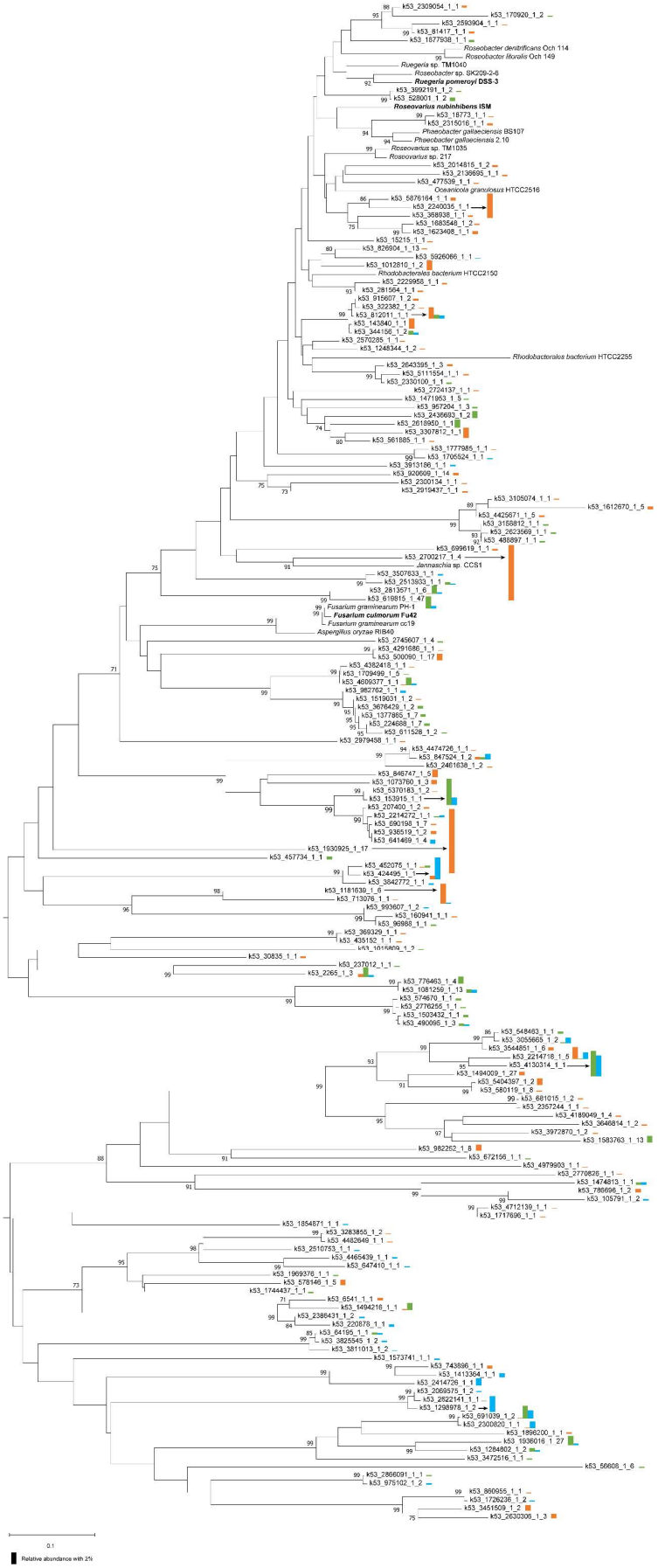
k53_2309054_1_1
k53_170920_1_2
k53_2593904_1_1
k53_81417_1_1
k53_1877938_1_1
Roseobacter denitrificans Och 114
Roseobacter litoralis Och 149
Ruegeria sp. TM1040
Roseobacter sp. SK209-2-6
Ruegeria pomeroyi DSS-3
k53_3992191_1_2
k53_528001_1_2
Roseovarius nubinhibens ISM
k53_18773_1_1
k53_2315016_1_1
Phaeobacter gallaeciensis BS107
Phaeobacter gallaeciensis 2.10
Roseovarius sp. TM1035
Roseovarius sp. 217
k53_2014815_1_2
k53_2136695_1_1
k53_477539_1_1
Oceanicola granulosus HTCC2516
k53_5876164_1_1
k53_2240035_1_1
k53_368938_1_1
k53_1683548_1_2
k53_1623408_1_1
k53_15215_1_1
k53_826904_1_13
k53_5926066_1_1
k53_1013810_1_2
Rhodobacterales bacterium HTCC2150
k53_2229958_1_1
k53_281564_1_1
k53_915607_1_2
k53_322382_1_2
k53_812011_1_1
k53_143840_1_1
k53_344156_1_2
k53_2570285_1_1
k53_1248344_1_2
Rhodobacterales bacterium HTCC2255
k53_2643395_1_3
k53_5111554_1_1
k53_2330100_1_1
k53_2724137_1_1
k53_1471853_1_5
k53_957204_1_3
k53_2436693_1_2
k53_2618950_1_1
k53_3307812_1_1
k53_561685_1_1
k53_1777985_1_1
k53_1705524_1_1
k53_3913186_1_1
k53_920609_1_14
k53_2300134_1_1
k53_2919437_1_1
k53_3105074_1_1
k53_1612670_1_5
k53_4425671_1_5
k53_3155812_1_1
k53_2623669_1_1
k53_488897_1_1
k53_699619_1_1
k53_2700217_1_4
Jannaschia sp. CCS1
k53_3507633_1_1
k53_2513933_1_1
k53_2813571_1_6
k53_619815_1_47
Fusarium graminearum PH-1
Fusarium culmorum Fu42
Fusarium graminearum cc19
Aspergillus oryzae RIB40
k53_2745607_1_4
k53_4291686_1_1
k53_500090_1_17
k53_4382418_1_1
k53_1709499_1_5
k53_4609377_1_1
k53_982762_1_1
k53_1519031_1_2
k53_3676429_1_2
k53_1377985_1_7
k53_224688_1_7
k53_611528_1_2
k53_2979458_1_1
k53_4474726_1_1
k53_647524_1_2
k53_2461638_1_2
k53_846747_1_5
k53_1073760_1_3
k53_5370183_1_2
k53_153915_1_1
k53_207400_1_2
k53_2214272_1_1
k53_690198_1_7
k53_936519_1_2
k53_641469_1_4
k53_1930925_1_17
k53_457734_1_1
k53_452075_1_1
k53_424495_1_1
k53_3842772_1_1
k53_1181639_1_6
k53_713078_1_1
k53_993607_1_2
k53_160941_1_1
k53_90988_1_1
k53_369329_1_1
k53_435152_1_1
k53_1019879_1_1
k53_30835_1_1
k53_237012_1_1
k53_2265_1_3
k53_776463_1_4
k53_1081256_1_13
k53_574670_1_1
k53_2776255_1_1
k53_1503432_1_1
k53_490095_1_3
k53_548463_1_1
k53_3055665_1_2
k53_3544851_1_6
k53_2214716_1_5
k53_4130314_1_1
k53_1494009_1_27
k53_5404397_1_2
k53_580119_1_8
k53_661015_1_2
k53_2357244_1_1
k53_4189049_1_4
k53_3646814_1_2
k53_3972870_1_2
k53_1583763_1_13
k53_982252_1_8
k53_672156_1_1
k53_4979903_1_1
k53_2770826_1_1
k53_1474813_1_1
k53_786596_1_2
k53_105791_1_2
k53_4712139_1_1
k53_1717696_1_1
k53_1854871_1_1
k53_3263855_1_2
k53_4482649_1_1
k53_2510753_1_1
k53_4465439_1_1
k53_647410_1_1
k53_1969376_1_1
k53_578146_1_5
k53_1744437_1_1
k53_8541_1_1
k53_1494216_1_1
k53_2386431_1_2
k53_220878_1_1
k53_64195_1_1
k53_3825545_1_2
k53_3811013_1_2
k53_1573741_1_1
k53_743896_1_1
k53_1413364_1_1
k53_2414726_1_1
k53_2069575_1_2
k53_2622141_1_1
k53_1298978_1_2
k53_691039_1_2
k53_2300820_1_1
k53_1896200_1_1
k53_1936016_1_27
k53_1284802_1_2
k53_3472516_1_1
k53_56608_1_6
k53_2866091_1_1
k53_975102_1_2
k53_860955_1_1
k53_1726236_1_2
k53_3451509_1_2
k53_2630306_1_3
0.1
Relative abundance with 2%

Fig. S15 Neighbor-Joining phylogenetic tree of DddP proteins from metagenome data. 182 protein sequences were used to construct the protein tree. The proteins shown to be functional marked with in bold. The topologies of phylogenetic tree were evaluated based on the bootstrap resampling method with 1000 replicates. Bootstrap coefficients below 70% were not shown. The relative abundance of protein sequences was indicated by bars. Orange bar, transition samples of summer. Green bar, transition samples of winter. The proteins shown to be functional were marked in bold.

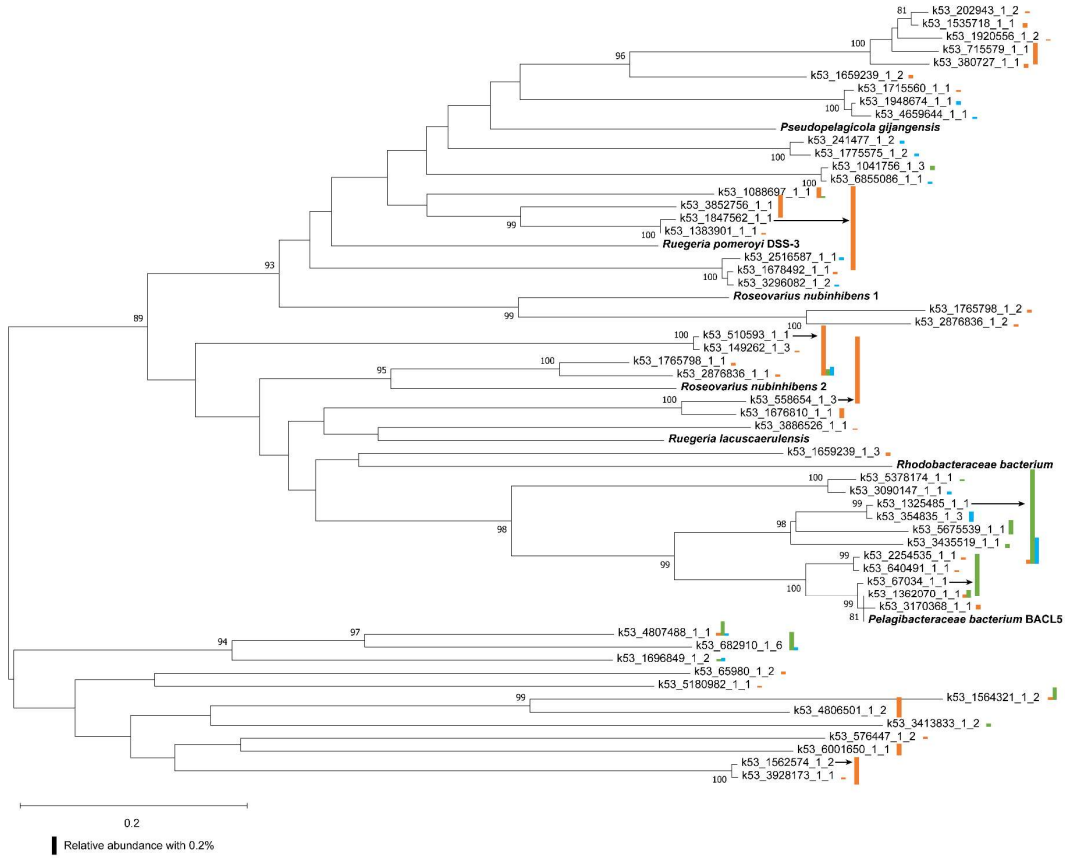

Fig. S16 Neighbor-Joining phylogenetic tree of DddQ proteins from metagenome data. 60 protein sequences were used to construct the protein tree. The proteins shown to be functional marked with in bold. The topologies of phylogenetic tree were evaluated based on the bootstrap resampling method with 1000 replicates. Bootstrap coefficients below 70% were not shown. The relative abundance of protein sequences was indicated by bars. Orange bar, transition samples of summer. Green bar, transition samples of winter. The proteins shown to be functional were marked in bold.

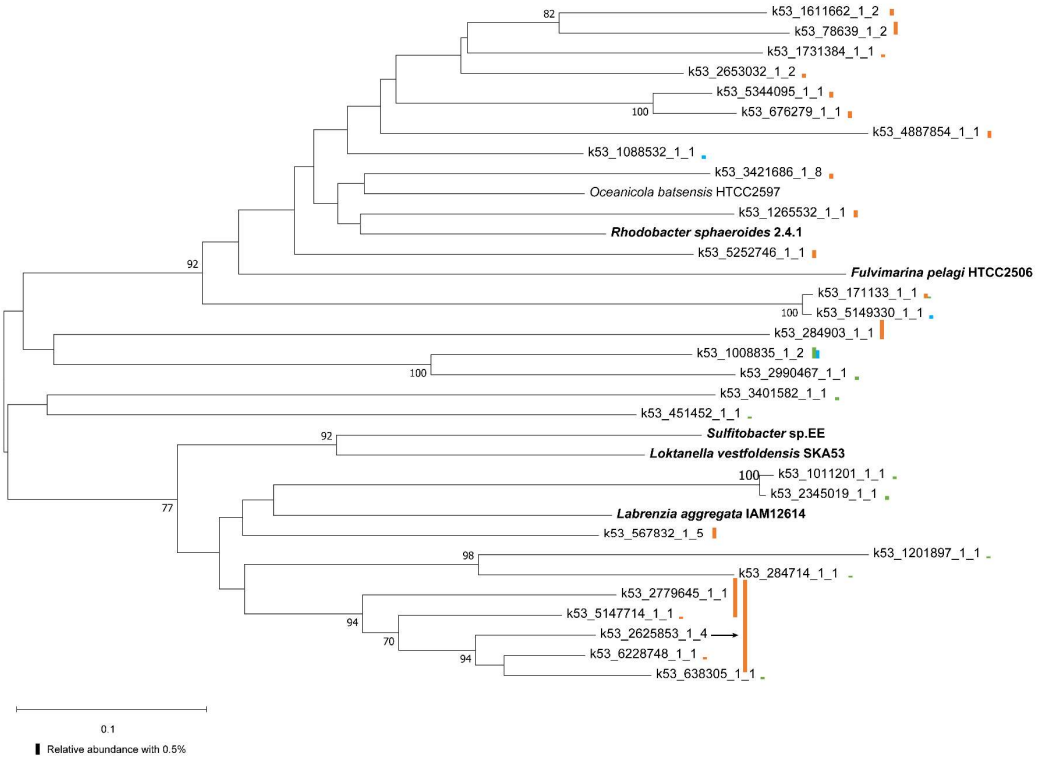

Fig. S17 Neighbor-Joining phylogenetic tree of DddL proteins from metagenome data. 34 protein sequences were used to construct the protein tree. The proteins shown to be functional marked with in bold. The topologies of phylogenetic tree were evaluated based on the bootstrap resampling method with 1000 replicates. Bootstrap coefficients below 70% were not shown. The relative abundance of protein sequences was indicated by bars. Orange bar, transition samples of summer. Green bar, transition samples of winter. The proteins shown to be functional were marked in bold.

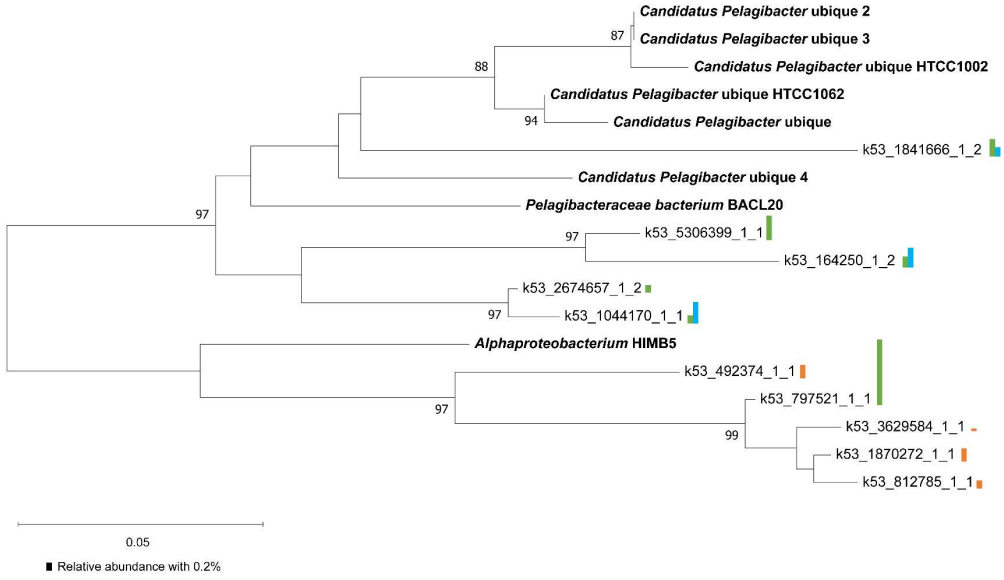

Fig. S18 Neighbor-Joining phylogenetic tree of DddK proteins from metagenome data. 18 protein sequences were used to construct the protein tree. The proteins shown to be functional marked with in bold. The topologies of phylogenetic tree were evaluated based on the bootstrap resampling method with 1000 replicates. Bootstrap coefficients below 70% were not shown. The relative abundance of protein sequences was indicated by bars. Orange bar, transition samples of summer. Green bar, transition samples of winter. Cyan bar, seawater samples of winter. The proteins shown to be functional were marked in bold.

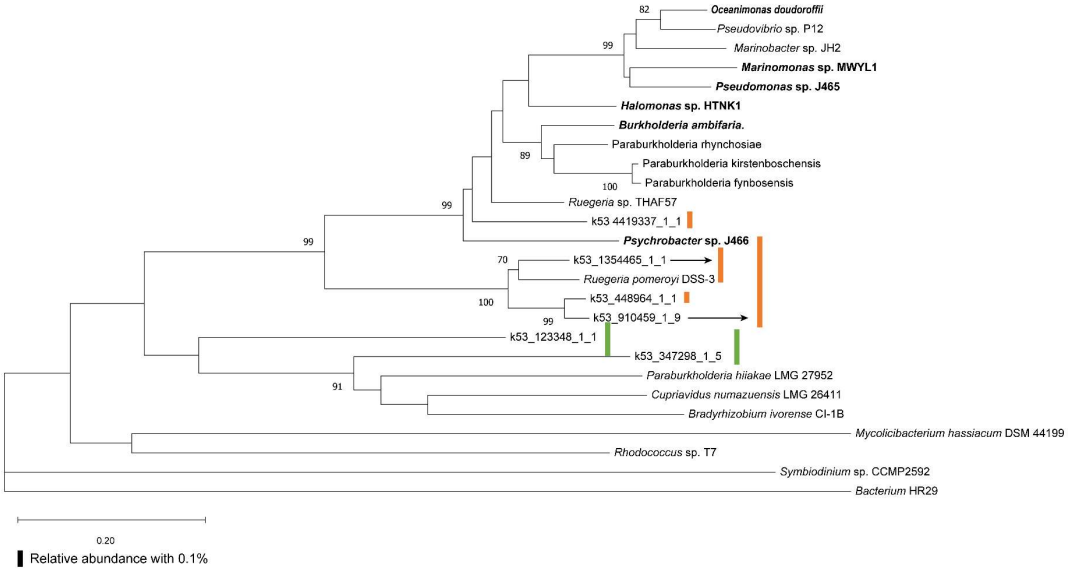

Fig. S19 Neighbor-Joining phylogenetic tree of DddD proteins from metagenome data. 25 protein sequences were used to construct the protein tree. The proteins shown to be functional marked with in bold. The topologies of phylogenetic tree were evaluated based on the bootstrap resampling method with 1000 replicates. Bootstrap coefficients below 70% were not shown. The relative abundance of protein sequences was indicated by bars. Orange bar, transition samples of summer. Green bar, transition samples of winter. The proteins shown to be functional were marked in bold.

Supplementary Tables

Table S1 Sampling sites and environmental factors of the Changjiang Estuary in winter

Station	Longitude (°E)	Latitude (°N)	Depth (m)	Salinity (PSU)	Temp (℃)	pH	DO (mg/l)	Chl *a* (μg/l)	SiO_3^{2-} (μM)	NO_2^- (μM)	NH_4^+ (μM)	PO_4^{3-} (μM)	NO_3^- (μM)	DMS (nM)	$DMSP_t$ (nM)	$DMSP_{p1}$ (nM)	$DMSP_{p2}$ (nM)	$DMSP_d$ (nM)
WC1S	121.11	31.75	1.01	0.16	9.82	8.06	11.33	0.67	106.65	2.30	0.16	1.81	129.08	-	2.26	1.09	0.08	1.10
WC1B	121.11	31.75	14.04	0.16	9.80	8.07	11.30	0.79	114.11	2.41	1.84	1.84	132.26	-	3.58	2.11	0.30	1.17
WC3S	121.32	31.57	1.01	0.16	9.82	8.00	11.24	0.72	109.66	2.24	N.D.	1.79	127.33	-	2.47	0.07	0.06	2.34
WC3B	121.32	31.57	18.86	0.17	9.88	8.00	11.25	0.81	112.12	2.46	0.13	1.97	141.12	-	5.83	1.21	1.95	2.66
WC5S	121.55	31.41	1.03	0.17	9.37	8.01	11.38	0.61	115.67	1.46	N.D.	1.82	144.05	-	1.77	0.22	0.42	1.14
WC5B	121.55	31.41	10.75	0.18	9.48	8.02	11.35	0.69	109.21	1.41	0.48	2.07	135.22	-	5.61	0.19	2.14	3.29
WC7S	121.79	31.24	1.01	0.39	9.41	7.77	10.90	0.99	98.45	2.55	3.26	1.86	165.09	-	0.95	0.11	0.46	0.38
WC7B	121.79	31.24	9.14	0.65	9.38	7.80	10.65	0.71	95.59	1.99	4.38	1.76	129.35	-	2.73	0.96	0.25	1.53
WA6-1S	122.07	31.06	1.01	19.86	8.11	7.98	10.98	0.32	40.24	0.31	6.12	0.82	56.57	-	3.12	1.00	1.95	0.16
WA6-1B	122.07	31.06	4.20	20.02	8.02	7.94	10.85	0.37	33.51	0.24	4.26	0.70	45.67	-	1.78	0.51	0.01	1.26
WA6-2S	122.25	30.95	1.01	23.66	8.12	7.94	10.62	0.36	44.20	0.23	5.32	1.13	51.23	-	4.47	2.93	0.55	0.99
WA6-2B	122.25	30.95	7.51	24.00	8.09	7.95	10.58	0.38	38.05	0.22	4.41	0.89	44.70	-	4.52	1.65	1.68	1.19
WA6-3S	122.38	30.90	1.03	27.93	8.90	8.03	10.19	0.30	23.84	0.15	3.08	0.71	26.71	-	12.33	8.56	1.84	1.94
WA6-3B	122.38	30.90	9.50	28.14	8.32	8.02	10.29	0.64	23.17	0.13	2.34	0.75	25.11	-	16.83	13.27	0.58	2.98
WA6-4S	122.50	30.87	1.01	29.52	8.79	8.08	10.05	0.30	17.73	0.21	7.30	0.60	19.37	-	9.11	2.02	2.78	4.31
WA6-4B	122.50	30.87	15.03	29.96	8.72	8.08	10.61	0.54	18.48	0.16	4.55	0.69	19.95	-	10.32	2.30	2.48	5.54

WA6-5S	122.61	30.84	1.03	30.17	9.88	8.02	N.D.	0.56	17.37	0.15	3.09	0.61	16.88	-	20.44	10.45	8.26	1.74
WA6-6S	122.83	30.78	1.01	30.37	8.87	8.08	10.03	0.32	16.65	0.17	3.46	0.60	17.25	-	5.68	1.05	0.86	3.78
WA6-5B	122.61	30.84	17.65	30.71	10.09	8.02	9.91	0.31	20.20	0.14	2.85	0.72	19.48	-	7.68	1.60	4.49	1.59
WA6-6B	122.83	30.78	21.42	32.67	10.25	8.10	9.46	0.24	12.85	0.12	3.71	0.57	11.12	-	6.34	2.89	0.45	3.00
WA6-7S	123.00	30.72	1.01	33.3	11.59	8.02	9.89	0.10	8.19	0.09	1.67	0.44	6.93	-	6.72	1.18	0.58	4.96
WA6-11S	123.99	30.41	1.05	33.90	12.85	8.07	9.06	0.31	6.62	0.32	1.71	0.39	4.56	-	5.14	0.09	3.47	1.58
WA6-11B	123.99	30.41	44.91	34.14	12.76	8.09	8.95	0.46	5.83	0.29	2.04	0.33	4.29	-	5.80	0.33	0.97	4.51
WA6-7B	123.00	30.72	47.72	34.25	13.82	8.02	8.74	0.26	8.18	0.16	2.64	0.43	6.17	-	4.62	0.19	2.86	1.57
WA6-10S	123.75	30.49	1.01	34.25	13.47	8.04	8.83	0.29	6.86	0.23	4.78	0.41	4.27	-	4.42	1.88	0.40	2.13
WA6-9S	123.50	30.56	1.05	34.29	14.28	8.06	8.68	0.31	5.91	0.13	1.75	0.36	4.05	-	3.47	0.07	2.92	0.48
WA6-10B	123.75	30.49	51.90	34.38	13.31	8.05	8.77	0.31	6.89	0.23	4.17	0.38	4.26	-	2.68	1.40	0.45	0.83
WA6-8S	123.25	30.64	1.01	34.49	14.48	8.07	8.61	0.20	5.66	0.16	4.59	0.36	3.65	-	4.84	0.45	0.51	3.88
WA6-9B	123.50	30.56	56.37	34.52	14.19	8.07	8.55	0.27	6.01	0.13	2.04	0.36	4.22	-	3.88	0.00	1.32	2.56
WA6-8B	123.25	30.64	62.01	34.62	14.42	8.07	8.55	0.22	4.68	0.14	4.53	0.32	3.31	-	5.91	0.76	0.13	5.02

***** Temp means temperature, N.D. means not detected, “W” means winter samples, “S” stands for surface seawater, “B” stands for bottom seawater.

***** $DMSP_t$, total DMSP. $DMSP_{p1}$, DMSP was these captured on 3 μm membrane. $DMSP_{p2}$, DMSP passed through 3 μm but was captured on the 0.22 μm filter. $DMSP_d$, dissolved DMSP.

***** The freshwater (salinity < 1 PSU), transitional area (1 PSU ≤ salinity < 30 PSU) and seawater (salinity ≥ 30 PSU).

Table S2 Sampling sites and environment factors of the Changjiang Estuary in summer

Station	Longitude (°E)	Latitude (°N)	Depth (m)	Salinity (PSU)	Temp (℃)	pH	DO (mg/l)	Chl *a* (μg/l)	SiO_3^{2-} (μM)	NO_2^- (μM)	NH_4^+ (μM)	PO_4^{3-} (μM)	NO_3^- (μM)	DMS (nM)	$DMSP_t$ (nM)	$DMSP_{p1}$ (nM)	$DMSP_{p2}$ (nM)	$DMSP_d$ (nM)
SC3B	121.32	31.57	19.00	0.11	28.84	7.84	5.69	0.55	113.64	0.17	0.12	1.37	99.14	1.77	5.06	3.82	0.04	1.20
SC1B	121.11	31.75	14.00	0.11	28.82	7.76	5.77	0.60	112.93	N.D.	N.D.	1.34	93.29	2.51	5.72	3.69	0.04	1.99
SC1S	121.11	31.75	1.00	0.11	28.96	7.84	5.87	1.34	111.65	N.D.	N.D.	1.32	98.54	1.97	7.56	2.87	4.61	0.09
SC3S	121.32	31.57	1.00	0.11	29.02	7.86	6.10	1.13	111.17	0.15	0.13	1.33	102.35	3.2	5.57	0.34	3.68	1.56
SC5S	121.56	31.40	1.00	0.11	29.17	7.80	5.82	1.75	113.38	0.11	N.D.	1.44	98.38	2.43	3.82	2.61	0.15	1.06
SC5B	121.56	31.40	16.00	0.11	28.92	7.76	5.55	0.84	114.56	0.22	0.25	1.40	101.26	3.63	5.81	0.30	5.38	0.14
SC7B	121.79	31.24	12.00	0.12	28.99	7.77	5.48	0.53	113.21	0.27	0.22	1.57	105.03	2.82	7.12	0.92	3.85	2.35
SC7S	121.79	31.24	1.00	0.12	29.03	7.80	5.65	0.99	110.78	0.31	0.26	1.58	98.67	5.63	11.15	4.18	2.61	4.37
SA6-1S	122.07	31.05	1.00	5.71	28.38	7.81	6.38	4.52	106.14	0.50	0.21	1.68	91.35	2.55	5.66	1.72	1.06	2.88
SA6-1B	122.07	31.05	8.00	6.87	28.28	7.72	6.30	1.64	107.26	0.35	1.33	1.67	91.14	0.97	7.49	3.15	1.59	2.75
SA6-2S	122.25	30.94	1.00	18.42	25.27	8.10	7.32	6.44	80.64	1.03	3.26	1.05	59.79	2.90	39.4	19.45	9.72	10.24
SA6-2B	122.25	30.94	10.00	19.81	24.82	7.88	5.11	3.14	67.08	1.01	3.59	1.18	53.51	1.29	9.21	6.51	0.83	1.88
SA6-3S	122.38	30.89	1.00	21.75	27.78	7.98	6.58	1.14	46.65	1.19	4.69	1.20	46.16	1.05	20.13	4.78	3.46	11.89
SA6-4S	122.49	30.87	1.00	25.88	25.96	7.94	5.92	0.97	36.29	1.56	6.1	1.03	34.06	0.90	32.18	10.81	2.97	18.41
SA6-5S	122.62	30.84	1.00	27.84	24.91	7.97	6.15	0.86	37.22	1.60	4.80	0.89	31.19	1.07	38.37	21.88	7.11	9.37
SA6-3B	122.38	30.89	13.00	27.90	24.52	7.95	5.54	0.61	40.69	1.31	4.77	1.11	38.03	0.99	22.24	9.66	5.87	6.71
SA6-7S	122.99	30.72	1.00	29.09	28.84	8.23	7.07	1.07	11.22	N.D.	5.96	0.08	6.97	6.75	22.03	14.87	3.61	3.54

SA6-6S	122.83	30.78	1.00	29.10	24.32	7.99	5.47	5.35	21.20	0.61	6.00	0.23	14.11	1.85	29.49	27.20	0.25	2.04
SA6-8S	123.24	30.64	1.00	29.5	29.26	8.26	7.46	1.39	5.99	0.19	6.78	ND	6.56	8.62	14.28	9.79	1.30	3.19
SA6-9S	123.49	30.56	1.00	30.98	29.53	8.3	7.13	1.97	0.74	0.21	7.33	0.06	1.13	4.95	9.74	7.49	0.70	1.55
SA6-4B	122.49	30.87	16.00	32.22	21.96	7.91	4.8	0.55	31.92	1.45	5.52	0.98	26.98	0.71	14.29	10.94	2.00	1.35
SA6-11S	123.98	30.41	1.00	33.36	N.D.	8.13	6.95	0.74	1.25	N.D.	6.63	0.06	N.D.	3.55	21.07	15.33	1.91	3.82
SA6-5B	122.62	30.84	20.00	33.44	21.01	7.89	4.1	0.73	25.56	1.39	5.6	0.91	19.19	1.06	19.30	17.03	0.23	2.05
SA6-10S	123.74	30.49	1.00	33.79	28.99	8.2	7.16	0.72	1.26	0.18	7.19	N.D.	0.75	6.85	10.44	8.66	0.43	1.36
SA6-11B	123.98	30.41	50.00	34.48	N.D.	7.97	4.93	0.45	8.95	0.41	7	0.54	4.75	1.43	8.93	6.88	0.58	1.46
SA6-9B	123.49	30.56	54.00	34.49	19.45	7.9	4.17	0.51	15.11	0.35	7.05	0.96	10.51	0.75	7.87	6.43	0.49	0.94
SA6-10B	123.74	30.49	54.00	34.5	21.16	7.95	4.39	0.39	11.97	0.52	6.71	0.79	7.55	0.96	12.03	8.96	2.20	0.87
SA6-8B	123.24	30.64	59.00	34.54	19.09	7.89	4.04	0.48	16.19	0.36	6.93	0.95	10.35	0.84	21.90	2.59	0.80	18.51
SA6-7B	122.99	30.72	46.00	34.55	19.8	7.89	3.69	0.32	17.11	0.45	7.44	1.02	10.78	1.00	20.42	5.01	1.71	13.69
SA6-6B	122.83	30.78	27.00	34.57	19.62	7.91	3.93	1.48	18.36	0.58	6.19	0.77	11.48	1.20	18.14	4.23	1.45	12.46

***** Temp means temperature, N.D., not detected, the former “S” means summer samples, the latter “S” stands for surface seawater; “B” stands for bottom seawater.

***** $DMSP_t$, total DMSP. $DMSP_{p1}$, DMSP was these captured on 3 μm membrane. $DMSP_{p2}$, DMSP passed through 3 μm but was captured on the 0.22 μm filter. $DMSP_d$, dissolved DMSP.

***** The freshwater (salinity < 1 PSU), transitional area (1 PSU ≤ salinity < 30 PSU) and seawater (salinity ≥ 30 PSU).

Table S3 The P value of statistical tests for the differences between seasons and among regions of environmental parameters.

Environmental parameters		Salinity	Temperature	pH	DO	Chl *a*	SiO_3^{2-}	NO_2^-	NH_4^+	PO_4^{3-}	NO_3^-	$DMSP_t$	$DMSP_{p1}$	$DMSP_{p2}$	$DMSP_d$
Seasons	Freshwater region	**0.000**	**0.000**	0.015	**0.000**			**0.001**		**0.000**	**0.000**	0.012	0.036		
	Transition region		**0.000**		**0.000**	**0.000**		**0.001**				**0.008**	0.013		0.026
	Seawater region		**0.000**		**0.000**	**0.000**		**0.000**	**0.000**	0.026		**0.000**	**0.000**		
Regions	Winter	**0.000**	**0.000**	0.020	**0.000**	**0.000**	**0.000**	**0.000**		**0.000**	**0.000**	0.031	0.031		
	Summer	**0.000**	**0.005**	**0.001**	0.031	**0.006**	**0.000**	**0.004**	**0.000**	**0.001**	**0.000**	**0.001**	**0.002**		0.023

***** Mann-Whitney tests were used for the seasonal differences in each region, and Kruskal-Wallis tests were used for regional differences in each season.

***** $DMSP_t$, total DMSP. $DMSP_{p1}$, DMSP was these captured on 3 μm membrane. $DMSP_d$, dissolved DMSP.

***** Only significant correlations were shown in table. Bold, $P < 0.01$; regular, $P < 0.05$

.

Table S4 The original read numbers of all samples, OTU numbers and diversity after rarefication

Samples	FL					PA				
	Original	OTU	Shannon	Chao 1	Coverage	Original	OTU	Shannon	Chao 1	Coverage
WC1B	N.D.	N.D.	N.D.	N.D.	N.D.	74136	681	2.69	1050.32	98.9%
WC1S	71162	947	3.67	1386.05	98.6%	67660	733	3.65	1051.50	98.9%
WC3S	N.D.	N.D.	N.D.	N.D.	N.D.	34821	935	4.72	1352.05	98.6%
WC3B	N.D.	N.D.	N.D.	N.D.	N.D.	57059	661	2.76	994.78	99.0%
WC5S	85684	543	5.34	554.00	99.9%	74403	646	3.48	1128.81	98.9%
WC5B	73950	1299	4.30	1978.53	97.9%	52161	855	2.28	1190.13	98.7%
WC7S	64377	1174	4.33	1852.59	98.1%	70530	721	2.25	1094.75	98.8%
WC7B	67745	1636	5.79	1900.93	98.5%	39064	785	2.14	1292.64	98.6%
WA6_1S	67134	1996	3.53	3126.15	96.3%	70472	799	2.04	1317.06	98.5%
WA6_1B	74268	2435	4.94	3445.06	96.2%	70058	256	4.70	280.00	99.9%
WA6_2S	54543	1854	2.97	3012.32	96.4%	49318	891	1.50	1692.81	97.9%
WA6_2B	74172	2285	3.95	3429.89	96.1%	70067	1728	2.61	2802.68	96.7%
WA6_3S	69803	1909	3.61	3046.24	96.5%	38791	704	1.58	1457.28	98.4%
WA6_3B	N.D.	N.D.	N.D.	N.D.	N.D.	30769	1361	1.82	2347.65	97.1%
WA6_4S	N.D.	N.D.	N.D.	N.D.	N.D.	48874	566	1.29	1095.73	98.8%
WA6_4B	50104	2434	5.55	2955.04	97.3%	56365	166	0.44	441.13	99.5%
WA6_5S	N.D.	N.D.	N.D.	N.D.	N.D.	49512	318	4.23	328.00	99.9%
WA6_6S	89404	1076	2.57	2266.31	97.7%	44412	769	3.24	1504.69	98.5%
WA6_5B	47202	1870	3.58	2881.94	96.5%	49771	868	1.70	1860.56	97.9%
WA6_6B	38680	1469	3.12	2356.60	97.2%	43025	914	4.83	1047.69	99.3%
WA6_7S	83771	974	2.72	2008.44	98.0%	31638	702	3.86	1250.44	98.8%
WA6_11S	80817	465	0.76	951.45	98.9%	36510	526	3.36	835.04	99.2%
WA6_11B	41900	1044	2.01	1720.84	97.9%	63447	476	2.84	711.30	99.3%
WA6_7B	56332	1249	3.27	2003.36	97.7%	74848	650	3.29	1075.01	98.9%
WA6_10S	85172	714	1.23	1328.09	98.5%	42438	554	3.25	984.62	99.1%
WA6_9S	83558	615	1.45	1263.31	98.6%	35799	571	3.25	831.68	99.2%
WA6_10B	30309	1017	2.45	1898.73	97.9%	50145	570	2.41	998.41	99.0%
WA6_8S	83463	630	1.69	1264.34	98.7%	38644	518	2.81	777.57	99.3%
WA6_9B	43509	1035	2.73	1638.19	98.1%	62144	489	2.49	745.20	99.3%
WA6_8B	33607	971	3.01	1606.89	98.2%	70573	748	4.71	1132.57	99.0%

SC3B	62758	875	3.56	1403.41	98.6%	41800	920	3.91	1290.74	98.7%
SC1B	73931	1006	4.13	1524.82	98.5%	37667	912	3.94	1418.36	98.6%
SC1S	N.D.	N.D.	N.D.	N.D.	N.D.	49684	902	3.89	1266.17	98.6%
SC3S	N.D.	N.D.	N.D.	N.D.	N.D.	43335	967	3.95	1541.55	98.5%
SC5S	74814	817	4.15	1146.39	98.9%	74434	847	3.15	1206.38	98.8%
SC5B	N.D.	N.D.	N.D.	N.D.	N.D.	63714	883	3.16	1324.50	98.6%
SC7B	58137	1237	4.20	1990.85	97.9%	43846	560	1.62	863.26	99.0%
SC7S	73131	1397	4.80	1859.37	98.0%	41719	1089	4.10	1736.60	98.2%
SA6_1S	89310	1489	5.14	2262.82	97.6%	34134	956	4.11	1488.79	98.5%
SA6_1B	66844	1229	2.74	2042.68	97.7%	62519	1427	5.06	2084.45	97.8%
SA6_2S	89909	949	3.29	1437.10	98.3%	35304	1040	4.38	1547.52	98.4%
SA6_2B	37770	1953	4.07	2954.87	96.6%	54826	1569	4.01	2639.82	97.0%
SA6_3S	86696	872	3.82	1421.43	98.5%	38887	746	3.70	1094.14	98.9%
SA6_4S	74397	832	2.89	1361.55	98.6%	59458	879	4.01	1350.30	98.6%
SA6_5S	87715	811	4.04	952.99	99.3%	38754	740	3.84	1137.07	98.8%
SA6_3B	64724	1297	4.09	2074.33	97.7%	47455	799	2.80	1261.31	98.6%
SA6_7S	94427	394	1.94	627.48	99.3%	59420	483	3.88	715.12	99.3%
SA6_6S	87932	610	2.29	970.62	98.9%	47999	619	3.60	996.37	99.0%
SA6_8S	88437	422	2.40	650.76	99.3%	50914	537	4.03	738.94	99.3%
SA6_9S	87649	516	1.74	676.58	99.3%	33862	383	3.53	515.22	99.5%
SA6_4B	32816	698	3.10	1173.26	98.8%	53371	716	3.15	1167.50	98.8%
SA6_11S	25418	507	1.99	571.68	99.6%	48787	529	3.34	698.47	99.4%
SA6_5B	55634	954	3.81	1533.57	98.4%	54515	772	3.29	1201.05	98.7%
SA6_10S	80615	423	1.58	690.99	99.2%	53039	560	3.48	835.31	99.2%
SA6_11B	70731	673	2.01	1103.68	98.7%	72541	763	3.90	1073.74	98.9%
SA6_9B	57422	643	1.88	745.03	99.3%	64059	866	4.10	1143.24	98.9%
SA6_10B	36588	798	2.85	1121.41	98.8%	50722	613	2.98	762.30	99.3%
SA6_8B	35438	878	3.65	1034.02	99.2%	69358	795	3.93	1180.03	98.9%
SA6_7B	84080	936	2.89	1457.95	98.3%	74175	955	3.98	1523.79	98.4%
SA6_6B	84684	909	3.29	1266.27	98.6%	70089	1068	4.23	1585.50	98.3%

* “W” means winter samples, the former “S” means summer samples, the latter “S” stands for surface seawater; “B” stands for bottom seawater.

* N.D., not detected. FL, free-living. PA, particle-associated.

Table S5 The numbers of gene homologues in the metagenomic samples.

	recA	*DSYB*	*dsyB*	*mmtN*	*Alma1*	*dddP*	*dmdA*	*TpMMT*	*dddY*	*dddK*	*dddW*	*dddQ*	*dddL*	*dddD*	*β-Actin*
SA6-2SFL	330	1	3	2	0	40	9	0	0	1	0	17	8	0	1
SA6-2BFL	319	0	3	0	0	30	13	0	0	2	0	14	6	0	3
SA6-6SFL	187	0	2	0	0	30	12	0	0	1	0	14	9	3	0
WA6-2SFL	241	1	5	0	0	34	11	0	0	4	0	8	4	1	5
WA6-2BFL	286	1	5	0	0	28	11	0	0	4	0	8	4	0	7
WA6-6SFL	220	2	7	0	0	35	9	0	0	2	0	15	3	0	5
SA6-2SPA	313	2	5	1	0	42	12	0	0	0	0	12	9	0	3
SA6-2BPA	325	0	5	0	0	38	10	0	0	2	0	19	6	0	0
SA6-6SPA	172	0	6	2	0	27	12	0	0	0	1	8	11	2	0
WA6-2SPA	308	0	4	1	0	40	13	0	0	0	0	6	8	0	0
WA6-2BPA	240	0	4	0	0	31	12	0	0	2	0	10	1	1	3
WA6-6BPA	261	0	9	0	0	40	17	0	0	2	0	11	4	0	6

FL, free-living. PA, particle-associated.

Table S6 Correlations between DMSP metabolic gene abundances in free-living bacteria and environmental factors.

Environment	Winter						Summer					
Factors	*dsyB*	*mmtN*	*dddP*	*dmdA*	*dmdA*(C/2)	*dmdA*(D/1)	*dsyB*	*mmtN*	*dddP*	*dmdA*	*dmdA*(C/2)	*dmdA*(D/1)
Longitude	0.398	0.454	**0.731**	**0.844**	**0.689**	**0.849**	**0.644**		**0.741**	**0.678**	**0.622**	**0.673**
Latitude	-0.398	-0.454	**-0.731**	**-0.844**	**-0.689**	**-0.849**	**-0.644**		**-0.741**	**-0.678**	**-0.622**	**-0.673**
Salinity	0.450	0.406	**0.707**	**0.808**	**0.691**	**0.807**	**0.722**		**0.736**	**0.644**	**0.689**	**0.640**
Temperature			**0.516**	**0.564**	**0.623**	**0.549**					-0.437	
pH			0.425	0.399		0.422	**0.507**		**0.749**	**0.764**	**0.641**	**0.766**
DO	**-0.492**	-0.418	**-0.716**	**-0.781**	**-0.649**	**-0.791**						
Chl *a*	**-0.494**	**-0.595**	**-0.525**	**-0.591**	**-0.498**	**-0.593**						
SiO_3^{3-}	-0.451	-0.374	**-0.729**	**-0.788**	**-0.666**	**-0.799**	**-0.688**		**-0.818**	**-0.746**	**-0.670**	**-0.742**
NO_2^-	**-0.491**	-0.409	-0.417	-0.448		-0.467				0.394	0.476	0.402
NH_4^+							**0.692**		**0.691**	**0.603**	**0.559**	**0.595**
PO_4^{3-}	-0.447		**-0.766**	**-0.790**	**-0.676**	**-0.795**	**-0.522**		**-0.782**	**-0.733**	**-0.669**	**-0.730**
NO_3^-	**-0.475**	-0.383	**-0.766**	**-0.806**	**-0.661**	**-0.817**	**-0.807**		**-0.833**	**-0.781**	**-0.734**	**-0.777**
$DMSP_t$	0.446								**0.600**	**0.653**	**0.693**	**0.661**
$DMSP_{p1}$					-0.394				**0.660**	**0.717**	**0.643**	**0.719**
$DMSP_d$										0.374	0.461	0.383

***** $DMSP_t$, total DMSP. $DMSP_{p1}$, DMSP was these captured on 3 μm membrane. $DMSP_d$, dissolved DMSP.

***** Only significant correlations were shown in table. Red, positive; blue, negative. Bold, $P < 0.01$; regular, $P < 0.05$.

Table S7 Correlations between DMSP metabolic gene abundances of particle-associated bacteria and environmental factors.

Environment	Winter						Summer					
Factors	*dsyB*	*mmtN*	*dddP*	*dmdA*	*dmdA*(C/2)	*dmdA*(D/1)	*dsyB*	*mmtN*	*dddP*	*dmdA*	*dmdA*(C/2)	*dmdA*(D/1)
Longitude		0.432			0.445		0.601					
Latitude		-0.432			-0.445							
Salinity		0.391		0.378	0.462		**0.752**					
pH			-0.369				0.397					
DO				-0.394	-0.428		**-0.484**		-0.420		-0.374	
Chl *a*	-0.387				-0.460		**-0.477**				-0.363	
SiO_3^{3-}		-0.391					**-0.612**					
NO_2^-	-0.419						0.417	0.440	**0.666**	**0.813**	**0.646**	**0.817**
NH_4^+	0.466				0.443		**0.636**					
PO_4^{3-}		-0.387			-0.477		**-0.637**					
DMS	N.D.	N.D.	N.D.	N.D.	N.D.	N.D.		-0.459	-0.595	-0.522	-0.435	-0.527
$DMSP_t$	0.460									0.398	0.428	0.391
$DMSP_{p1}$	0.476											
$DMSP_d$										0.454	0.423	0.449

* $DMSP_t$, total DMSP. $DMSP_{p1}$, DMSP was these captured on 3 μm membrane. $DMSP_d$, dissolved DMSP. N.D., no DMS data.

* Only significant correlations were shown in table. Red, positive; blue, negative. Bold, $P < 0.01$; regular, $P < 0.05$.

Table S8 The reference DMSP producing and catabolic genes used in the metagenomic analysis

Genes	Gene accession numbers	Protein accession numbers	Strains
dsyB	-	EEL96501	*Bacillus mycoides* DSM204
dsyB	-	CTQ43687	*Labrenzia aggregata* CECT
dsyB	-	AOR83342	*Labrenzia aggregata* LZB0
dsyB	-	ERP98606	*Labrenzia* sp. C1B10
dsyB	-	ERR00112	*Labrenzia* sp. C1B70
dsyB	-	WP_051644456	*Labrenzia* sp. DG1229
dsyB	-	WP_043143384	*Mameliella alba* UMTAT08
dsyB	-	WP_043748339	*Pseudooceanicola atlanticu*
dsyB	-	WP_023852424	*Rhodobacteraceae bacteriu*
dsyB	-	WP_025312975	*Roseibacterium elongatum*
dsyB	-	WP_030879264	*Streptomyces varsoviensis*
dsyB	2620496472	-	*Antarctobacter heliothermu*
dsyB	2517908241	-	*Amorphus coralli* DSM197
dsyB	2520173307	-	*Caenispirillum salinarum* A
dsyB	2616590712	-	*Citreicella aestuarii* DSM2
dsyB	2514595470	-	*Citreicella* sp. 357
dsyB	2579689465	-	*Defluviimonas* sp. 20V17
dsyB	2553022978	-	*Donghicola* sp. S598
dsyB	639943763	-	*Labrenzia aggregata* IAM1
dsyB	2517312627	-	*Labrenzia alexandrii* DFL1
dsyB	2616591799	-	*Litorimicrobium taeanense*
dsyB	648280724	-	*Maritimibacter alkaliphilus*
dsyB	2525377636	-	*Nisaea denitrificans* DSM1
dsyB	641429164	-	*Nisaea* sp. BAL199
dsyB	638883374	-	*Pseudooceanicola batsensis*
dsyB	2558678304	-	*Pseudooceanicola nanhaier*
dsyB	2541035415	-	*Oceanicola* sp. HL-35
dsyB	2527024186	-	*Oceanicola* sp. S124
dsyB	648285806	-	*Salipiger bermudensis* HTC
dsyB	2524485630	-	*Pseudodonghicola xiamene*
dsyB	2609135787	-	*Rhizobiales bacterium* HL1
dsyB	2609105254	-	*Rhodobacteraceae bacteriu*
dsyB	2593183274	-	*Rhodospirillales bacterium*
dsyB	2597124009	-	*Roseibium hamelinense* AT
dsyB	2565720611	-	*Roseivivax halodurans* JCM
dsyB	2635168442	-	*Roseivivax sediminis* DSM2
dsyB	2620334468	-	*Roseovarius indicus* DSM2
dsyB	640641694	-	*Sagittula stellata* E37
dsyB	2523510257	-	*Salipiger mucosus* DSM160
dsyB	2523943366	-	*Sediminimonas qiaohouens*
dsyB	2525928126	-	*Stappia stellulata* DSM588
dsyB	2599852567	-	*Thalassobaculum litoreum*

dsyB	2523405058	-	*Thalassobaculum salexigen*
dsyB	2622865483	-	*Thalassobius gelatinovorus*
dsyB	2623181840	-	*Tropicibacter naphthaleniv*
dsyB	2617877652	-	*Yangia pacifica* CGMCC13
dsyB	2620103054	-	*Yangia pacifica* DSM26894
mmtN	-	WP_052321947	*Novosphingobium* sp. MBE
mmtN	-	WP_066775518	*Croceicoccus mobilis* strain
mmtN	-	WP_044830103	*Thalassospira* sp. HJ NODE
mmtN	-	WP_062957385	*Thalassospira* sp. MCCC 1A
mmtN	-	WP_064788038	*Thalassospira indica* strain
mmtN	-	WP_064780488	*Thalassospira tepidiphila* M
mmtN	-	WP_033070178	*Thalassospira australica* str
mmtN	-	WP_022734010	*Thalassospira lucentensis* M
mmtN	-	WP_063085993	*Thalassospira* sp. MCCC 1A
mmtN	-	WP_008888945	*Thalassospira profundimari*
mmtN	-	WP_068409229	*Labrenzia* sp. OB1
mmtN	-	WP_064261696	*Roseovarius indicus* strain H
mmtN	-	WP_057814729	*Roseovarius indicus* strain D
mmtN	-	KRS18724	*Roseovarius indicus* strain H
mmtN	-	WP_076485456	*Rhodobacter aestuarii* strain
mmtN	-	WP_033429235	*Saccharothrix syringae* stra
mmtN	-	WP_091090849	*Micromonospora nigra* stra
mmtN	-	WP_071204336	*Agrobacterium vitis* strain N
mmtN	-	WP_017624909	*Nocardiopsis chromatogene*
mmtN	-	EME99407	*Streptomyces mobaraensis*
dddP	-	ZP_00959238	*Roseovarius nubinhibens* IS
dddP	-	ZP_01755203	*Roseobacter* sp. SK209-2-6
dddP	-	ZP_01741265	Rhodobacteraceae bacterium
dddP	-	ZP_02144167	*Phaeobacter gallaeciensis* D
dddP	-	ZP_02150063	*Phaeobacter gallaeciensis* 2
dddP	-	ZP_01881042	*Roseovarius* sp. TM1035
dddP	-	ZP_01036399	*Roseovarius* sp. 217
dddP	-	YP_682809	*Roseobacter denitrificans* O
dddP	-	ZP_02139379	*Roseobacter litoralis* Och14
dddP	-	YP_167522	*Ruegeria pomeroyi* DSS-3
dddP	-	ZP_01156882	*Oceanicola granulosus* HTC
dddP	-	ZP_01448542	Rhodobacterales bacterium
dddP	-	YP_509721	*Jannaschia* sp. CCS1
dddP	>XM_001823859	XP_001823911	*Aspergillus oryzae* RIB40
dddP	>EU_784955	ACF19794	*Gibberella zeae* strain cc19
dddP	>XM_389272	XP_389272	*Gibberella zeae* PH-1
dddP	>EU_784956	ACF19795	*Fusarium culmorum* strain D
dddP	-	YP_613011	*Ruegeria* sp. TM1040
dmdA	-	AAV95190	*Ruegeria pomeroyi* DSS-3
dmdA	-	ABF64177	*Ruegeria* sp.TM1040
dmdA	-	ABD55296	*Jannaschia* sp. CCS1

dmdA	-	EAP76657	*Roseovarius nubinhibens* IS
dmdA	-	EAQ43549	*Roseobacter* sp. MED193
dmdA	-	EBA11882	*Roseobacter* sp. CCS2
dmdA	-	EAQ26389	*Roseovarius* sp. 217
dmdA	-	YP_001533657	*Dinoroseobacter shibae* DF
dmdA	-	EBA17661	*Roseobacter* sp. SK209-2-6
dmdA	-	EBA02880	*Rhodobacteraceae bacteriu*
dmdA	-	ABG31871	*Roseobacter denitrificans* C
dmdA	-	EDM32633	*Roseovarius* sp. TM1035
dmdA	-	EDM71141	*Roseobacter* sp. AzwK-3b
dmdA	-	EAU51039	Rhodobacterales bacterium
dmdA	-	AAZ21068	*Pelagibacter ubique* HTCC
dmdA	-	EAW42451	Gmmaproteobacterium HT
dmdA	-	EDP61332	Alphaproteobacterium BAL
Alma1	-	XP_005784450	*Emiliania huxleyi* CCMP15
Alma1	-	XP_005763983	*Emiliania huxleyi* CCMP15
TpMMT	-	XP_002296942	*Thalassiosira pseudonana* C
TpMMT	-	XP_002286764	*Thalassiosira pseudonana* C